

AD-A188 456

MORPHOLOGICAL STUDIES OF CONDUCTIVE POLYMERS(U)  
ROCKWELL INTERNATIONAL THOUSAND OAKS CA SCIENCE CENTER  
J WALKER ET AL 31 MAY 87 NADC-87092-68

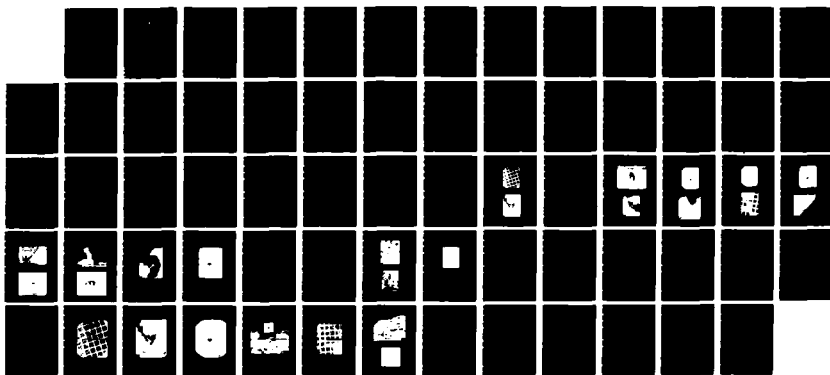
1/1

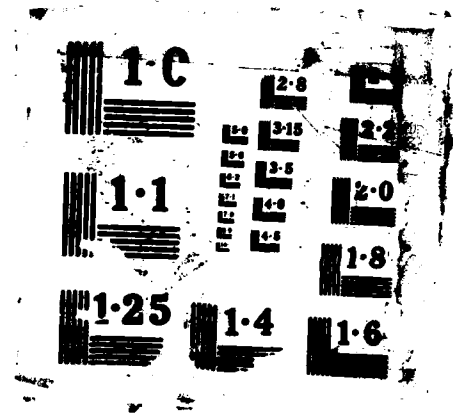
UNCLASSIFIED

N62269-85-C-0269

F/G 7/6

NL





DTIC FILE COPY

REPORT NO. NADC-87092-60

AD-A188 456



## MORPHOLOGICAL STUDIES OF CONDUCTIVE POLYMERS

ROCKWELL INTERNATIONAL SCIENCE CENTER  
1049 Camino Dos Rios  
Thousand Oaks, CA 91360

MAY 31, 1987

Contract No. N62269-85-C-0269

DTIC  
ELECTED  
NOV 23 1987  
**S** **D**  
*A* *H*

Approved For Public Release;  
Distribution Is Unlimited

Prepared For  
Air Vehicle and Crew Systems  
Technology Department (Code 8064)  
NAVAL AIR DEVELOPMENT CENTER  
Warminster, PA 18974-5000

87 11 9 015

## NOTICES

**REPORT NUMBERING SYSTEM** - The numbering of technical project reports issued by the Naval Air Development Center is arranged for specific identification purposes. Each number consists of the Center acronym, the calendar year in which the number was assigned, the sequence number of the report within the specific calendar year, and the official 2-digit correspondence code of the Command Office or the Functional Department responsible for the report. For example: Report No. NADC-88015-70 indicates the fifteenth Center report for the year 1988 and prepared by the Systems and Software Technology Department. The numerical codes are as follows:

CODE	OFFICE OR DEPARTMENT
00	Commander, Naval Air Development Center
01	Technical Director, Naval Air Development Center
02	Comptroller
05	Computer Department
07	Planning Assessment Resources Department
10	Anti-Submarine Warfare Systems Department
20	Tactical Air Systems Department
30	Battle Force Systems Department
40	Communication & Navigation Technology Department
50	Mission Avionics Technology Department
60	Air Vehicle & Crew Systems Technology Department
70	Systems & Software Technology Department
80	Engineering Support Group

**PRODUCT ENDORSEMENT** - The discussion or instructions concerning commercial products herein do not constitute an endorsement by the Government nor do they convey or imply the license or right to use such products.

8a. NAME OF FUNDING / SPONSORING ORGANIZATION Naval Air Development Center	8b. OFFICE SYMBOL (if applicable) 606	9. PROCUREMENT INSTRUMENT IDENTIFICATION NUMBER Contract No. N62269-85-C-0269		
8c. ADDRESS (City, State, and ZIP Code)  Warminster, PA 18974		10. SOURCE OF FUNDING NUMBERS  PROGRAM ELEMENT NO. WR22-06      PROJECT NO. E01      TASK NO. N/A      WORK UNIT ACCESSION NO. N/A		
11. TITLE (Include Security Classification)  (U) Morphological Studies of Conductive Polymers				
12. PERSONAL AUTHOR(S) J. Walker and L.J. Buckley				
13a. TYPE OF REPORT Final	13b. TIME COVERED FROM 9/23/85 TO 4/24/87	14. DATE OF REPORT (Year, Month, Day)		15. PAGE COUNT 61
16. SUPPLEMENTARY NOTATION				
17. COSATI CODES  FIELD    GROUP    SUB-GROUP		18. SUBJECT TERMS (Continue on reverse if necessary and identify by block number)  Conductive Polymers, TEM, X-Ray Diffraction		
19. ABSTRACT (Continue on reverse if necessary and identify by block number)  A series of free-standing films of doped polypyrrole were prepared and characterized by x-ray and electron diffraction methods. The degree of order observed in these films was found to be dependent upon the incorporated dopant anions and polymer synthesis conditions. Thus, the benzenesulfonate monoanions and the long chain alkyl sulfates were found to promote the formation of the highest order polypyrrole films. Transmission Electron Microscope (TEM) observation of these polymers confirmed that the most ordered polymers contained a greater degree of crystallinity than the least ordered polymers. A cyclic voltammetric technique for assessing the order in thin polypyrrole films is described. Other conducting polymers were also characterized by diffraction techniques. Thus, polypyrrole prepared by the ferric ion oxidation of pyrrole monomer, was much less ordered than the corresponding electrodeposited polymers. X-ray and electron diffraction techniques were employed to evaluate the morphology of doped poly-3-methylthiophene. The 3-methyl substituent apparently renders the lattice of this polymer more ordered and less flexible than the corresponding polypyrrole structure.				
20. DISTRIBUTION / AVAILABILITY OF ABSTRACT <input type="checkbox"/> UNCLASSIFIED/UNLIMITED <input checked="" type="checkbox"/> SAME AS RPT. <input type="checkbox"/> DTIC USERS		21. ABSTRACT SECURITY CLASSIFICATION UNCLASSIFIED		
22a. NAME OF RESPONSIBLE INDIVIDUAL Dr. L Buckley		22b. TELEPHONE (Include Area Code) 215-441-2383	22c. OFFICE SYMBOL 6064	

## TABLE OF CONTENTS

	<u>Page</u>
<b>SUMMARY .....</b>	viii
<b>INTRODUCTION .....</b>	1
<b>1.0 POLYPYRROLE .....</b>	2
1.1 Experimental .....	4
1.2 Polypyrrole Film Synthesis .....	5
1.2.1 Preparation of Naphthalenedisulfonyl Chlorides (2,6 and 2,7 Isomers) .....	6
1.2.2 Hydrolysis of Aromatic Sulfonyl Chlorides .....	6
1.2.3 Preparation of Tetraalkylammonium Salts of Aromatic Sulfonates .....	8
1.3 Diffraction Measurements .....	8
1.4 Results and Discussion .....	9
1.4.1 X-Ray Diffraction .....	9
1.4.2 Transmission Electron Microscopy .....	23
1.5 Conclusions .....	35
<b>2.0 CHEMICALLY DEPOSITED POLYPYRROLE.....</b>	36

## TABLE OF CONTENTS

	<u>Page</u>
<b>3.0 POLY-3-METHYLTHIOPHENE .....</b>	<b>39</b>
<b>3.1 Introduction .....</b>	<b>39</b>
<b>3.2 Experimental .....</b>	<b>39</b>
<b>3.3 Results and Discussion .....</b>	<b>40</b>
<b>3.3.1 Poly-3-methylthiophene Film Synthesis.....</b>	<b>40</b>
<b>3.3.2 X-Ray Diffraction.....</b>	<b>40</b>
<b>3.3.3 Transmission Electron Microscopy .....</b>	<b>43</b>
<b>3.3.4 Conclusions .....</b>	<b>45</b>
<b>4.0 REFERENCES .....</b>	<b>52</b>

## LIST OF FIGURES

<u>Figure</u>		<u>Page</u>
1	Proposed structure for oxidized polypyrrole .....	2
2	Model structure for an ordered and random polymer .....	3
3	Proposed model for the short-range order in the polypyrrole (PPY)-tenside salts, seen along the polypyrrole chains axis. The simple black lines represent the PPY chains; the zig-zag lines symbolize the alkyl chains of the tensides and the black circles stand for the ionic $-SO_3^-$ or $-OSO_3^-$ groups; for d(n) .....	4
4	Polypyrrole 2-naphthalene sulfonate (NpSO <sub>3</sub> ); 0.1M pyrrole; pH = 1.7; Au electrode; $\sigma = 49 \Omega^{-1}\text{-cm}^{-1}$ .....	5
5	Polypyrrole trichlorobenzenesulfonate (TCBSH); 0.1M pyrrole; 2% H <sub>2</sub> O/ACN; ITO electrode; $\sigma = 87 \Omega^{-1}\text{-cm}^{-1}$ .....	10
6	Polypyrrole dodecylbenzene sulfonate, 0.1M dodecylbenzene sulfonic acid; 0.1M pyrrole; pH = 2.1; Au electrode, $\sigma = 30 \Omega^{-1}\text{-cm}^{-1}$ .....	12
7	Polypyrrole dodecylsulfate (DDS); 0.1M Na DDS; 0.1M pyrrole; pH = 7.6; Au electrode, $\sigma = 48 \Omega^{-1}\text{-cm}^{-1}$ .....	12
8	Polypyrrole tosylate (TOS); 0.2M HTOS; 0.15M pyrrole; pH = 1.8; Au electrode, $\sigma = 65 \Omega^{-1}\text{-cm}^{-1}$ .....	13
9	Polypyrrole tosylate; 0.2M HTOS (ACN); 0.15M pyrrole; PG, $\sigma = 2 \Omega^{-1}\text{-cm}^{-1}$ .....	13
10	Polypyrrole 1,2 Ethane Disulfonate (EDS Na <sub>2</sub> ); 0.1M pyrrole; Au electrode, $\sigma = 7.9 \Omega^{-1}\text{-cm}^{-1}$ .....	14
11	Polypyrrole Monochlorobenzenesulfonate (MCBSH); 0.1M MCBSH; 0.1M pyrrole; ITO electrode, $\sigma = 120 \Omega^{-1}\text{-cm}^{-1}$ .....	14
12	Polypyrrolechloride, 0.3M HCl (water); 0.1M pyrrole; Au electrode, $\sigma = 9.2 \Omega^{-1}\text{-cm}^{-1}$ .....	15
13	Polypyrrole methane sulfonate (MES); 0.1M HMES; 0.1M pyrrole; Au electrode, $\sigma = 2 \Omega^{-1}\text{-cm}^{-1}$ .....	15
14	Polypyrrole polystyrene sulfonate (PSSA); 0.1M PSSA; 0.1M pyrrole; pH = 1.9; Au electrode, $\sigma = 8 \Omega^{-1}\text{-cm}^{-1}$ .....	16

For \_\_\_\_\_

I II III IV V VI VII VIII 

By _____	Distribution/ _____
Availability Codes	
Dist _____	Avail and/or Special _____
A-1	_____



## LIST OF FIGURES (Continued)

<u>Figure</u>		<u>Page</u>
15	<b>Polypyrrole 1,5-NDS; 0.1M 1,5-NaNDS; 0.1M pyrrole; PG electrode, <math>\sigma = 14 \Omega^{-1}\text{-cm}^{-1}</math> .....</b>	16
16	<b>Polypyrrole 2,6-naphthalene sulfonate (NDS); 0.1M Na 2,6NDS; 0.1M pyrrole; pH = 6.6; Au electrode, <math>\sigma = 75 \Omega^{-1}\text{-cm}^{-1}</math> .....</b>	17
17	<b>Hypothetical polypyrrole segment .....</b>	18
18	<b>First reduction cycle of as-deposited polypyrrole tosylate thin films, evaluated in deoxygenated 0.1M aqueous sodium tosylate (dotted curve) and in 0.1M tetraethylammonium tetrafluoroborate in acetonitrile (solid curve), scan rate 50 mV/s, film thickness corresponds to 40 mC/cm<sup>2</sup> of charged passed, pwhh = peak width at half height .....</b>	22
19	<b>TEM photograph of electrodeposited polypyrrole tosylate .....</b>	25
20	<b>TEM photograph of electrodeposited polypyrrole tosylate .....</b>	25
21	<b>Diffraction pattern from discrete particles on continuous film .....</b>	27
22	<b>TEM photograph of electrodeposited polypyrrole DDS .....</b>	27
23	<b>TEM photograph of electrodeposited polypyrrole DDS .....</b>	28
24	<b>TEM photograph of electrodeposited polypyrrole DDS .....</b>	28
25	<b>Electron diffraction pattern electrodeposited polypyrrole DDS .....</b>	29
26	<b>TEM photograph of electrodeposited polypyrrole DDBS .....</b>	29
27	<b>Electron diffraction pattern of electrodeposited polypyrrole DDBS .....</b>	30
28	<b>TEM photograph of a thin film of polypyrrole MCBS with crystalline grains .....</b>	30
29	<b>Dark field TEM photograph of polypyrrole MCBS showing crystalline grains .....</b>	31
30	<b>Diffraction pattern from thin film of polypyrrole MCBS .....</b>	31

## LIST OF FIGURES (Continued)

<u>Figure</u>		<u>Page</u>
31	TEM photograph of polypyrrole PCBS; film is agglomeration of spheroids .....	32
32	Diffraction pattern from spheroids of polypyrrole PCBS .....	32
33	TEM photograph of polypyrrole TCBS .....	33
34	Diffraction pattern from fiber of polypyrrole TCBS .....	34
35	TEM photograph of chemically deposited polypyrrole triflate .....	37
36	TEM photographs of chemically deposited polypyrrole triflate .....	37
37	TEM photograph of chemically deposited polypyrrole triflate .....	38
38	X-ray diffraction pattern of poly(3-methylthiophene) trifluoromethanesulfonate prepared at 0-5°C from propylene carbonate .....	42
39	X-ray diffraction pattern of poly(3-methylthiophene) trifluoromethanesulfonate prepared at -40°C from propylene carbonate .....	42
40	X-ray diffraction pattern of poly(3-methylthiophene) perfluorooctylsulfonate prepared from propylene carbonate .....	44
41	Magnified view of poly-3-methylthiophene triflate grown upon a TEM grid grown from 0.1M [Bu <sub>4</sub> N] CF <sub>3</sub> SO <sub>3</sub> in acetonitrile .....	46
42	Larger magnification of the polymer shown in previous figure .....	47
43	Electron diffraction pattern produced by the polymer shown in previous figure .....	48
44	Magnified view of a poly-3-methylthiophene triflate grown from 0.1M CF <sub>3</sub> SO <sub>3</sub> H in acetonitrile .....	49
45	TEM photograph of poly-3-methylthiophene perfluorooctylsulfonate deposited from propylene carbonate .....	50
46	Magnified view of poly-3-methylthiophene hexafluorophosphate grown from propylene carbonate .....	51

## SUMMARY

The following is a summary of research performed under the above contract. The objectives of this research were: (1) to develop methods for the solid-state characterization of electrodeposited conducting polymers, and then (2) to determine the relationships between the overall polymer synthesis conditions and the observed polymer morphology with respect to the various physical properties such as dc conductivity, density and thermal stability. The determination of the morphology or microstructure of these materials and the factors that influence their microstructures may help to explain their complicated nature. Further, such information is important to the production of semiconducting polymeric materials for device applications, especially those having anisotropic electrical and optical properties. The techniques used for the solid-state characterization of these solids were x-ray diffraction and transmission electron microscopy.

The technique of x-ray diffraction has been identified as a method of characterizing the relative degree of order that exists in the many derivatives of the conducting polymer, polypyrrole. On the basis of an extensive study on the morphology of polypyrrole as influenced by the incorporated dopant ion and synthesis conditions, we can conclude that the structure of the dopant anion exerts a pronounced effect on the microstructure of this polymer. These effects are manifested in the physical properties of the polymer, e.g., bulk conductivity, surface morphology, tensile strengths and chemical/thermal stability. The x-ray diffraction results indicate that the pyrrole polymers containing aromatic sulfonate monoanions appear to exhibit the highest degree of order, while those polymers containing the smaller anions or dianions appear largely amorphous.

Transmission Electron Microscopy (TEM) was investigated as an alternate means of determining the degree of crystallinity present in polypyrrole derivatives and to provide a means of measuring the crystal lattice parameters of these derivatives. Several methods of TEM sample preparation were investigated. The best TEM samples were prepared by using a gold TEM grid as the anode in the polymer electro-depositions. The most crystalline polypyrrole derivatives as judged by TEM, contain either the

dodecylsulfate or trichlorobenzenesulfonate anions. The low degree of order present in most of the polypyrrole derivatives prevents the accurate determination of polymer lattice parameters.

We present a new technique which we have developed jointly with Rockwell IR&D, for the determination of the relative degree of order in thin films of electrodeposited polypyrrole. This method is based upon the voltammetric response curves of the as deposited polypyrrole thin films. The degree of polymer order, as determined by diffraction techniques, correlates with the peak width of the first cathodic scan of the polypyrrole thin films. This method appears to be a simple and reliable technique for rapid screening of structural order in polypyrrole-dopant systems.

Polypyrrole, prepared chemically by the ferric ion oxidation of the pyrrole monomer, was characterized by TEM and SEM techniques. These materials are also of low crystallographic order, however, an interesting polymer growth morphology is observed for these polymers. High magnification TEM microscopy reveals that the chemically prepared polymers consist of individual hexagonal or octagonal particles about 1000Å in diameter. These particles probably arise from polymerization of the monomer on the surface of the individual crystallites of the ferric salt.

Other electrodeposited conducting polymers were also examined by TEM and x-ray diffraction. Electrodeposited poly-3-methylthiophene triflate is observed to be more ordered than the corresponding hexa-fluorophosphate derivative. This polymer system, unlike the polypyrroles, cannot be prepared electrochemically with many of the larger dopant anions. This may relate to the higher degree of order and consequently less flexible structure of the polythiophene derivatives.

## INTRODUCTION

This report is organized into several sections. Each section is a self-contained entity including experimental, results and discussion section. The polymer morphology and physical properties of the following conducting polymer systems were investigated:

- (1) Electrodeposited polypyrrole
- (2) Chemically deposited polypyrrole
- (3) Electrodeposited poly-3-methylthiophene.

## 1.0 POLYPYRROLE

The considerable interest in the electrically conducting polymer polypyrrole, stems from its high conductivity, ease of preparation and environmental stability of its doped forms.<sup>1</sup> Polypyrrole, which can be synthesized by either chemical or electrochemical techniques, is formed by the simultaneous oxidation and polymerization of pyrrole monomer. The structure of the polymer formed by such methods is thought to contain a cationic backbone of pyrrole monomer units linked in a regular fashion through the alpha carbon atoms. The positive charge of the polymer is compensated by the inclusion of dopant anions. Thus, the as-synthesized polypyrrole is a molecular composite (see Fig. 1) of a cationic polymer backbone and the corresponding number of dopant anions required to maintain charge neutrality.

SC40265

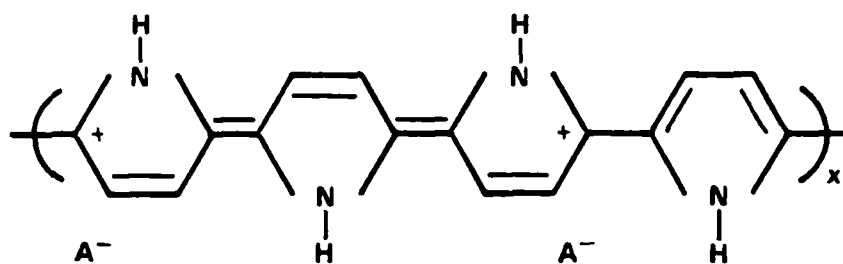


Fig. 1 Proposed structure for oxidized polypyrrole.

The mode of electrical conduction in polypyrrole is still an issue. The most widely accepted view of electron transport in conducting polymers involves the idea of electron hopping from one closely associated polymer chain to another.<sup>2</sup> This notion suggests that the arrangement of the individual polymer chains within the polymer structure should play a significant role in the determination of the electrical properties of polypyrrole. For example, the electrical properties of a fully ordered polymer, as depicted in Fig. 2, should be different than those of a randomly oriented polymer. As seen from Fig. 2, the packing of the polymer chains in the solid is influenced not only by

the geometric characteristics of the monomer units but also by the dopant anion size and shape. It follows that the ability of the polymer to adopt an ordered structure depends upon the compatibility of the dopant anion with the lattice of the ordered polymer.

SC40244

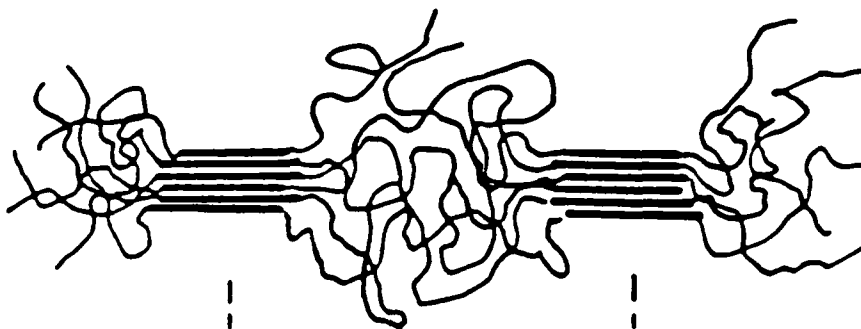


Fig. 2 Model structure for an ordered and random polymer.

While much data is now available on the electrical properties of polypyrrole, relatively little is known about the polymer structure or how the polymer structure is influenced by the incorporated dopant anion and/or polymer synthesis conditions. Wegner has examined films of polypyrrole tensides by x-ray diffraction and speculated that the polymer chains form a kind of double-layered structure as shown in Fig. 3.<sup>3</sup> Mitchell has suggested that the chains of polypyrrole tosylate adopt a planar conformation and that the counterions lie in the plane of the polymer. It was further stated that the processing conditions affect the nature of the molecular anisotropy in the electrochemically prepared polypyrrole.<sup>4</sup> The purpose of this section of the program was to develop methods for the study of the solid state structure of polypyrrole and to use these techniques, namely, x-ray diffraction and transmission electron microscopy, to evaluate the morphologies and relative order of a series of free-standing polypyrrole films deposited under a variety of experimental conditions. In the course of these studies observations made on the cyclic voltammetric characteristics of thin films of electrodeposited polypyrrole have provided an additional means for evaluating the order in polypyrrole. Presented below are the results of these studies.

SC40245

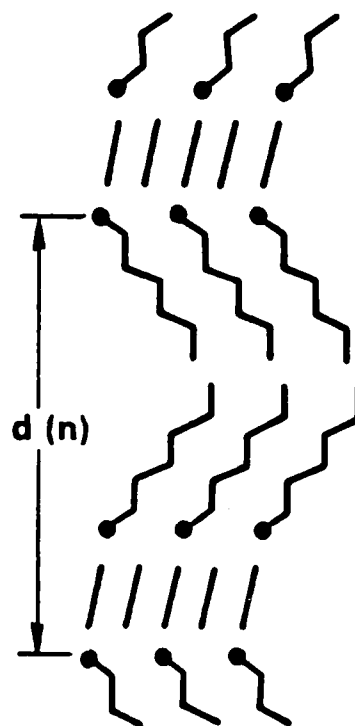


Fig. 3 Proposed model for the short-range order in the polypyrrole (PPY)-tenside salts, seen along the polypyrrole chains axis. The simple black lines represent the PPY chains; the zig-zag lines symbolize the alkyl chains of the tensides and the black circles stand for the ionic  $-SO_3$  or  $-OSO_3$  groups; for  $d(n)$ .

### 1.1 Experimental

Pyrrole monomer (Aldrich) was distilled under nitrogen and stored in a closed container in a refrigerator. All solvents were high purity reagents that were commercially obtained. Electrodepositions were performed using a PAR model 173 Potentiostat/Galvanostat equipped with a PAR model 179 coulombmeter. Standard deposition conditions for producing films of polypyrrole are presented in Table 2. The thick, free-standing polypyrrole films were deposited from a two or three electrode cell. The working electrode was either a  $28\text{ cm}^2$  gold-plated copper sheet (masked on the edges and back), a rectangular sheet of conducting ITO glass, or a square of pyrolytic

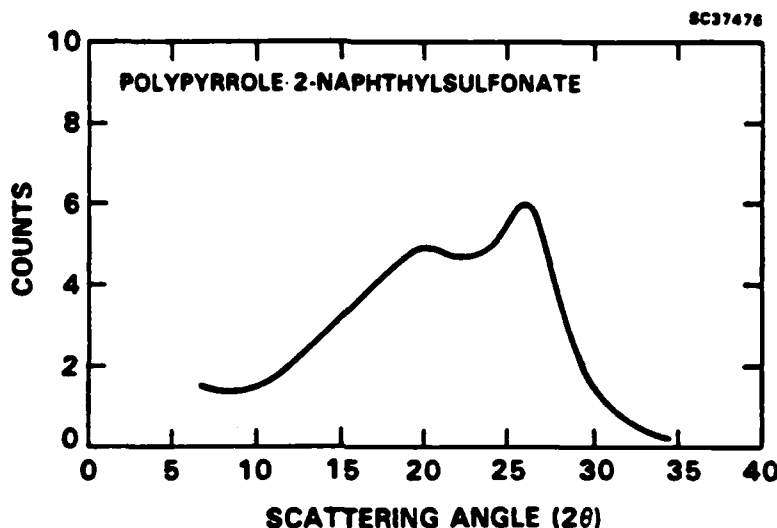


Fig. 4 Polypyrrole 2-naphthalene sulfonate ( $\text{NpSO}_3$ ); 0.1M pyrrole; pH = 1.7; Au electrode;  $\sigma = 49 \Omega^{-1}\text{-cm}^{-1}$ .

graphite. The counter electrode was either a sheet of pyrolytic graphite, a sheet of gold-plated nickel, or a cylindrical platinum mesh electrode. The reference electrode, if used, was either SCE for aqueous depositions or a platinum wire for deposition from acetonitrile. Films were deposited at current densities between 1.8 to 3.6  $\text{mA/cm}^2$  at constant current. The films were deposited until charge equivalent to 20-25 coulombs/ $\text{cm}^2$  was passed. Deposition solutions were approximately 0.1M both in pyrrole and supporting electrolyte. No precautions were taken to exclude oxygen from the cells. The films were removed from the electrodes and rinsed thoroughly with water or acetonitrile depending upon which solvent was used. The films were dried at ambient temperature and stored in a refrigerator. Electrolytes were obtained commercially (Aldrich or Alfa) or when necessary synthesized using the procedures described below. DC conductivities were determined with a four-point probe apparatus (Alessi Industries).

## 1.2 Polypyrrole Film Synthesis

Smooth, black, free-standing films of polypyrrole were prepared by anodic oxidation of pyrrole monomer in a single compartment electrochemical cell, using two or

three electrodes. The polymer films were typically deposited at a constant current from either aqueous or acetonitrile solutions of the monomer and electrolyte. Presented in Table 1, are the relevant deposition conditions used in the preparation of the polymer films along with the dopant ion structures and conductivities for the respective polymer films. As can be seen from this table, a large variety of dopant ions have been successfully incorporated into polypyrrole. The structural diversity of the dopants ranges from small compact ions, such as chloride or triflate, to long aliphatic ions, such as dodecylsulfate or dodecylbenzenesulfonate. As will be seen, the dopant ion structure plays a decisive role in the determination of the relative order in polypyrrole.

#### 1.2.1 Preparation of Naphthalenedisulfonyl Chlorides (2,6 and 2,7 Isomers)

Fifteen ml of thionyl chloride were added to an ice-cooled suspension of 25.0 g (0.075 mol) of the appropriate naphthalenedisulfonic acid disodium salt in 80 ml dimethylformamide. This mixture was stirred and allowed to warm to room temperature overnight. The reaction was quenched by adding 500 ml of crushed ice to the mixture. The precipitated solid was collected by filtration, rinsed twice with water, and dried in a vacuum oven overnight. The 2,7 isomer was purified by two recrystallizations from dichloromethane-cyclohexane producing 13.7 g (56%) of pure product (mp 155-156°C). The 2,6 isomer was purified by recrystallization from toluene producing 15.9 g (65%) of pure product (mp 223-225°C).

#### 1.2.2 Hydrolysis of Aromatic Sulfonyl Chlorides

The conversion of aromatic sulfonyl chlorides to the corresponding sulfonic acids is accomplished by suspending the sulfonyl chloride in deionized water. The reaction mixtures are stirred and maintained at 65-75°C until a homogeneous solution is obtained. This generally requires 12 to 48 h. The free acids can be isolated by evaporation of the water and dessication of the residue. In most cases, the free acid can then be directly converted to crystalline tetraalkylammonium salts by the following procedure.

**Table I**  
**Deposition Conditions for Thick, Freestanding**  
**Polypyrrole Films for X-ray Evaluation**

ELECTROLYTE*	DOPANT ANION STRUCTURE	SOLVENT	ANODE	CURRENT COULOMBS CONDUCTIVITY			SC40229
				1000	1000	10 <sup>-1</sup> cm <sup>-1</sup>	
MSH	<chem>[CH3]SC(=O)[O-]</chem>	H <sub>2</sub> O	Au	80 mA	1000	1.6	
TSN	<chem>[CH3-C6H4-]SC(=O)[O-]</chem>	H <sub>2</sub> O	Au	100 mA	1000	121	
TSNa	<chem>[Na+-C6H4-]SC(=O)[O-]</chem>	H <sub>2</sub> O	Au	100 mA	1000	43	
BSP	<chem>[C6H5-]SC(=O)[O-]</chem>	2%H <sub>2</sub> O/ACN	ITO	24 mA	332	81	
NSH	<chem>[C6H5-CH2-]SC(=O)[O-]</chem>	ACN H <sub>2</sub> O	PG Au	17 mA 100 mA	275 1000	78 80	
NaDDS	<chem>[C12H25OSO3]^-</chem>	H <sub>2</sub> O	Au	80 mA	1000	18	
DDDSH	<chem>[C12H25-C6H4-]SC(=O)[O-]</chem>	H <sub>2</sub> O	Au	125 mA	2240	29	
1,8NDSNa2	<chem>[O-][C6H4-]2[SC(=O)[O-]]2</chem>	H <sub>2</sub> O	Au	125	1262	26	
2,6NDSNa2	<chem>[O-][C6H3(O)-]2[SC(=O)[O-]]2</chem>	H <sub>2</sub> O	Au	100 mA	1076	74	
2,7NDSNa2	<chem>[O-][C6H4-]2[SC(=O)[O-]]2</chem>	H <sub>2</sub> O	Au	100 mA	1081	91	
MCSH	<chem>[C6H4-]SC(=O)[O-]</chem>	2%H <sub>2</sub> O/ACN	ITO	24.8 mA	282	120	
TCBSH	<chem>[C6H4-]2SC(=O)[O-]</chem>	2%H <sub>2</sub> O/ACN	ITO	37 mA	578	87	
PCBSH	<chem>[C6H4-]2SC(=O)[O-]</chem>	2%H <sub>2</sub> O/ACN	ITO	24 mA	247	40	
mBDSH2	<chem>[O-][C6H4-]2[SC(=O)[O-]]2</chem>	H <sub>2</sub> O	PG	17.3 mA	200	32	
BPDSH2	<chem>[O-][C6H4-]2[C6H4-]2[SC(=O)[O-]]2</chem>	7%H <sub>2</sub> O/ACN	ITO	30 mA	273	18	
EDSNa2	<chem>[O-][C6H4-]2[SC(=O)[O-]]2</chem>	H <sub>2</sub> O	Au	100 mA	760	7.0	
PSSH	<chem>[C6H4-]2SC(=O)[O-]</chem>	H <sub>2</sub> O	Au	125 mA	2123	9.4	

MSH = METHANESULFONIC ACID. BSH = BENZENESULFONIC ACID. TSN = TOLUENESULFONIC ACID.  
 TSNa = SODIUM TOSYLATE. NSH = 2-NAPHTHYSULFONIC ACID. NaDDS = SODIUM DODECYLSULFONATE.  
 DDDSH = DODECYLBENZENESULFONATE. 2,6NDSNa2 = SODIUM 2,6-NAPHTHYLDISULFONATE. 2,7NDSNa2  
 = SODIUM 2,7-NAPHTHYLDISULFONATE. MCSH = 4-CHLOROBENZENESULFONIC ACID. TCBSH = 2,4,5-  
 TRICHLOROBENZENESULFONIC ACID. PCBSH = PENTACHLOROBENZENESULFONIC ACID.  
 mBDSH2 = META-BENZENE-DISULFONIC ACID. BPDSH2 = 4,4'-BIPHENYLDISULFONIC ACID.  
 EDSNa2 = SODIUM 1,3-ETHANEDISULFONATE. PSSH = POLYSTYRENESULFONIC ACID

### 1.2.3 Preparation of Tetraalkylammonium Salts of Aromatic Sulfonates

To a solution of the appropriate sulfonic acid in water, we added a solution containing one equivalent of the tetraalkylammonium hydroxide in the case of a monosulfonate and two equivalents in the case of a disulfonate. Towards the end of the addition, the pH of the solution was monitored with pH paper. The hydroxide solution was added until the reaction mixture reached a pH of 7. The solvent was evaporated on a roto-vap and the residue dried in vacuo. The salts were typically recrystallized from acetone-hexane or methylene chloride-tetrahydofuran solvent mixtures.

### 1.3 Diffraction Measurements

Most x-ray diffraction measurements were made using a Diano 53XRD-8530 semiautomatic x-ray diffractometer. X-ray diffraction traces obtained on this instrument were digitized using a Hewlett-Packard digitizing tablet. Other measurements were performed at the NADC x-ray facility in Warminster, PA. Transmission Electron Microscopy was performed on a Phillips 75EM-400 electron microscope equipped with a high tilt goniometer specimen stage and heating and cooling specimen stages. Polypyrrole samples for TEM evaluation were electro-deposited onto gold grids (500 mesh) in a three electrode cell. A  $0.75 \text{ cm}^2$  platinum sheet was used for the counter electrode, while a silver/silver nitrate/tetraethylammonium tetrafluoroborate/acetonitrile electrode was used for the reference. The area of the gold grid was calculated to be about  $0.3 \text{ cm}^2$ . The grid, gripped by a gold-plated clip, was partially immersed into the electrolyte solution. A constant anodic current of about  $1 \text{ mA/cm}^2$  was applied to the grid. Deposition was interrupted at different times and the deposit evaluated under a microscope for the presence of polymer nodules in the grid holes. Deposition was terminated when the presence of nodules or needles was detected and thought to provide samples of sufficient quality for TEM evaluation.

**Table 2**  
**Deposition Parameters for the Preparation of**  
**Polypyrrole Samples for TEM Evaluation**

Electrolyte*	Solvent	Current	Coulombs
HTMBS	ACN	200 uA	58 mC
HTCBS	ACN	ne record of deposition	
H2mBDS	ACN	280 uA	35 mC
HPCBS	6%H <sub>2</sub> O/ACN	280 uA	45 mC
TEAT	ACN	280 uA	47 mC
HMCBS	ACN	280 uA	40 mC
NaDDS	H <sub>2</sub> O	280 uA	23 mC
H2BPDS	7%H <sub>2</sub> O/ACN	250 uA	500 mC

\*HTMBS = 1,3,5-trimethylbenzenesulfonic acid; HTCBS = trichlorobenzenesulfonic acid; H2mBDS = meta-benzene-disulfonic acid; HPCBS = pentachlorobenzenesulfonic acid; TEAT = tetraethylammonium tosylate; HMCBS = para-chlorobenzenesulfonic acid; NaDDS = sodium dodecylsulfate; H2BPDS = 4,4'-biphenyl-isulfonic acid; ACN = acetonitrile.

#### 1.4 Results and Discussion

##### 1.4.1 X-Ray Diffraction

X-ray scattering measurements were made using Cu K<sub>α</sub> radiation together with a diffractometer operating in the scan mode. In general, the polypyrrole films give rise to x-ray diffraction patterns that exhibit a broad distribution of scattered intensity around  $2\theta = 20$  deg. The shape and intensity of this scattering is observed to be highly dopant ion dependent. For example, the diffraction pattern obtained from a film of polypyrrole 2-naphthylsulfonate (Fig. 4) appears to consist of two overlapping peaks between  $10 < 2\theta < 30$  deg, the lower angle peak broader than the higher angle peak. In contrast, the polypyrrole film containing the trichlorobenzenesulfonate (Fig. 5) anion gives rise to single broad diffraction peak between  $20 < 2\theta < 30$  deg. Displayed in

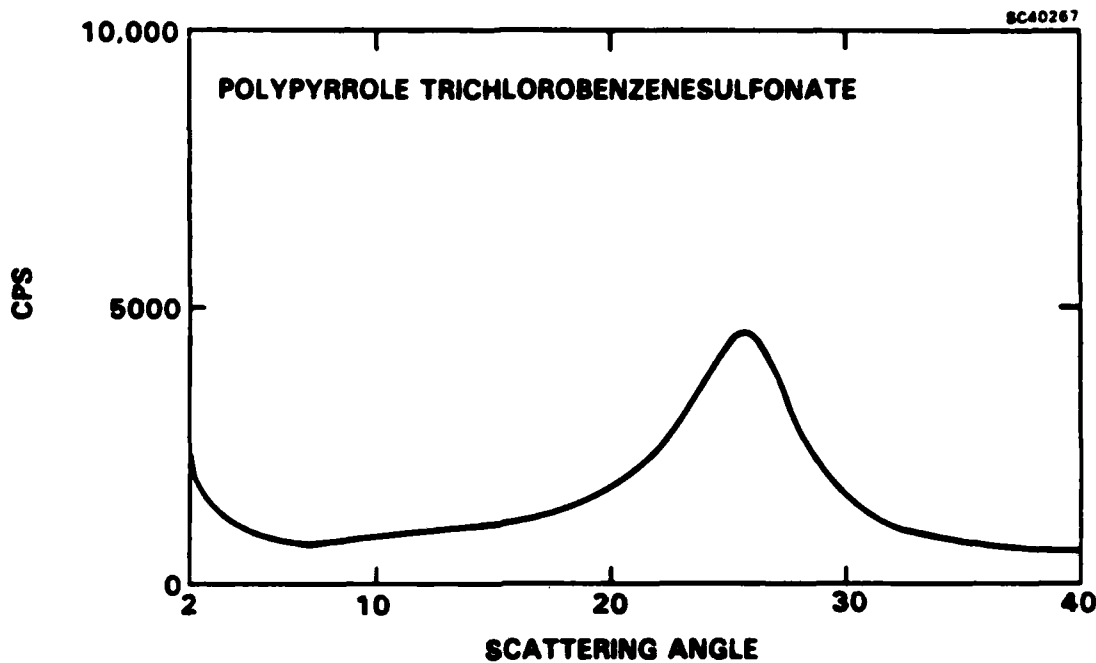


Fig. 5 Polypyrrole trichlorobenzenesulfonate (TCBSH); 0.1M pyrrole; 2% H<sub>2</sub>O/ACN; ITO electrode;  $\sigma = 87 \Omega^{-1}\text{-cm}^{-1}$ .

Figs. 4-16, are the x-ray diffraction curves for the polypyrrole films that were prepared. Collected in Table 3, are diffraction maxima for all of the films that were analyzed as well as the corresponding d-spacings and an indication of peak multiplicity.

An unusual feature of some of the diffraction patterns was the observation of a low angle peak between  $3 < 2\theta < 7$  deg. This feature is clearly illustrated in the x-ray scattering curve obtained from a film of polypyrrole dodecylbenzenesulfonate deposited from aqueous solution (Fig. 6). This film exhibits a broad low angle peak at  $2\theta = 3.46$  deg. Polypyrrole films doped with dodecylsulfate (Fig. 7) and tosylate (Figs. 8 and 9) exhibit qualitatively similar x-ray diffraction patterns.

**Table 3**  
**X-Ray Diffraction Data for Electrodeposited Polypyrrole Films**

Dopant-Ion	Peak Maxima (°)	d-Spacing (Å)
Dodecylbenzenesulfonate	3.9 22.5	22.65
Polystyrenesulfonate	21.0	4.23
Dodecylsulfate	4.0 20.5	22.08
2-Naphthylsulfonate	20.0 26.5	4.44
2,6-Naphthalenedisulfonate	26.25	3.39
Methanesulfonate	7.0 17.0 20.5 24.0	12.62 5.21 4.33 3.71
Tosylate (water)	5.1 20.5	17.33 4.33
Tosylate (ACN)	21.25	4.18
1,5-Naphthalenedisulfonate	17.1 26.0	5.21 3.42
Chloride	26.1	3.41
Trichlorobenzenesulfonate	26.0	3.42
Monochlorobenzenesulfonate	26.1	3.41

On the basis of the observed x-ray diffraction patterns it is apparent that there are two mutually dependent types of solid state order present in the doped polypyrrole films. The first type is associated with the degree of order of the polymer backbone. The degree of this order is reflected by the peak width and peak height of the higher angle ( $15 < 2\theta < 30$  deg) diffraction peak. The second type of ordering present in the polypyrrole films is associated with the incorporated dopant ions. The extent of this order is manifested by the peak width and height of the lower angle diffraction peaks ( $3 < 2\theta < 7$  deg).

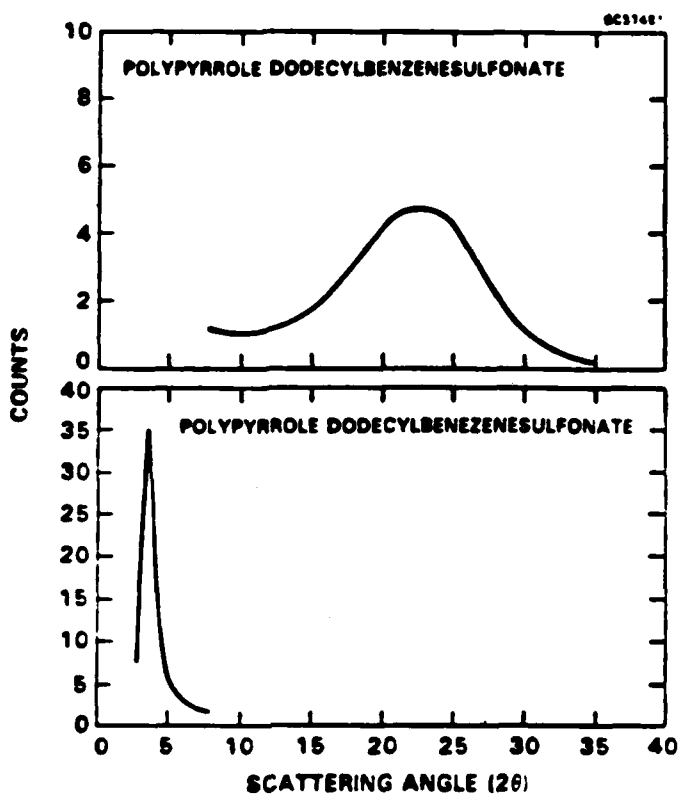


Fig. 6 Polypyrrole dodecylbenzene sulfonate, 0.1M dodecylbenzene sulfonic acid; 0.1M pyrrole; pH = 2.1; Au electrode,  $\sigma = 30 \Omega^{-1}\text{-cm}^{-1}$ .

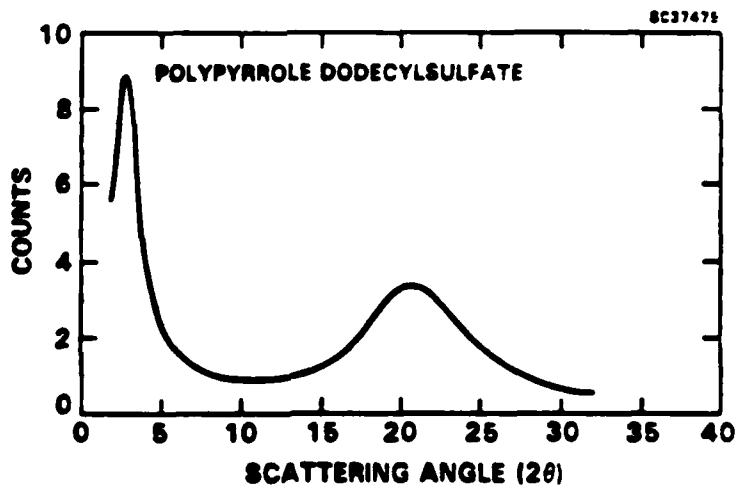


Fig. 7 Polypyrrole dodecylsulfate (DDS); 0.1M Na DDS; 0.1M pyrrole; pH = 7.6; Au electrode,  $\sigma = 48 \Omega^{-1}\text{-cm}^{-1}$ .

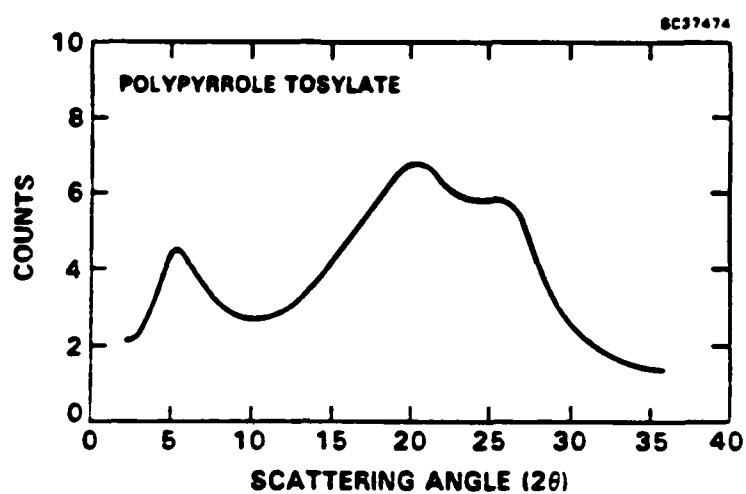


Fig. 8 Polypyrrole tosylate (TOS); 0.2M HTOS; 0.15M pyrrole; pH = 1.8; Au electrode,  $\sigma = 65 \Omega^{-1}\text{-cm}^{-1}$ .

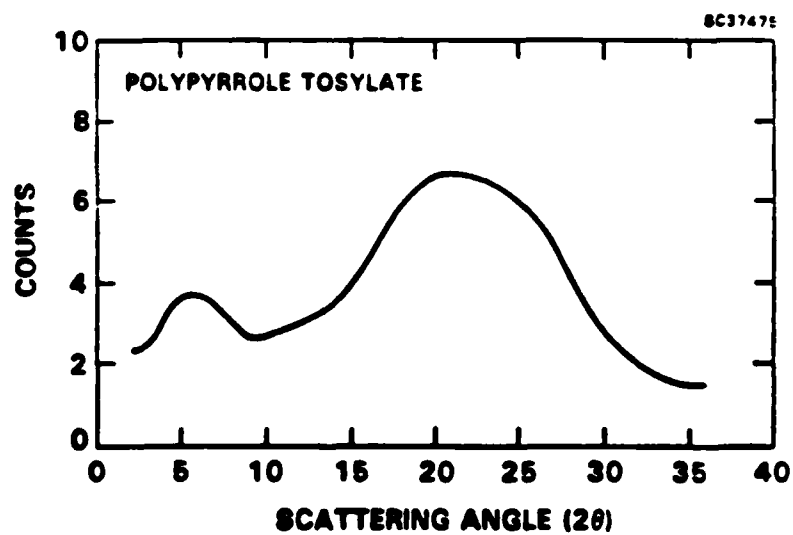


Fig. 9 Polypyrrole tosylate; 0.2M HTOS (ACN); 0.15M pyrrole; PG,  $\sigma = 2 \Omega^{-1}\text{-cm}^{-1}$ .

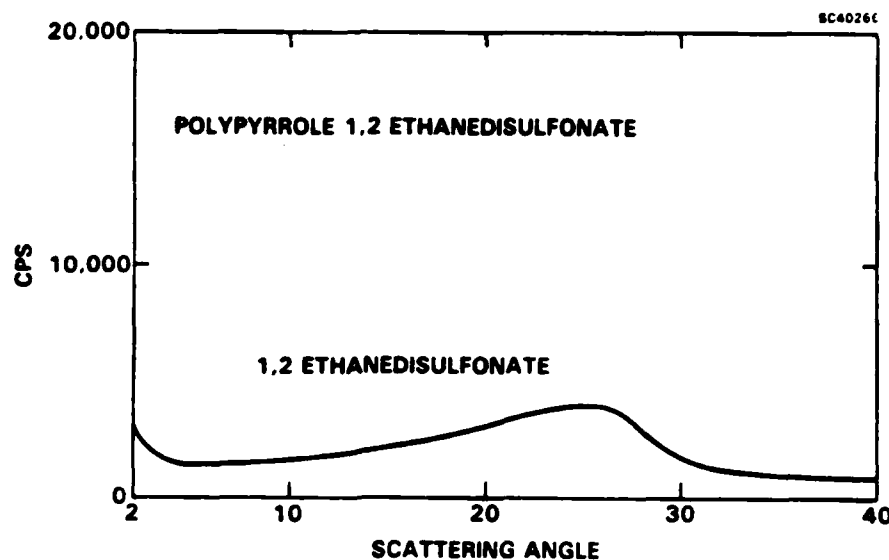


Fig. 10 Polypyrrole 1,2 Ethane Disulfonate ( $\text{EDSNa}_2$ ); 0.1M pyrrole; Au electrode  
 $\sigma = 7.9 \Omega^{-1}\text{-cm}^{-1}$ .

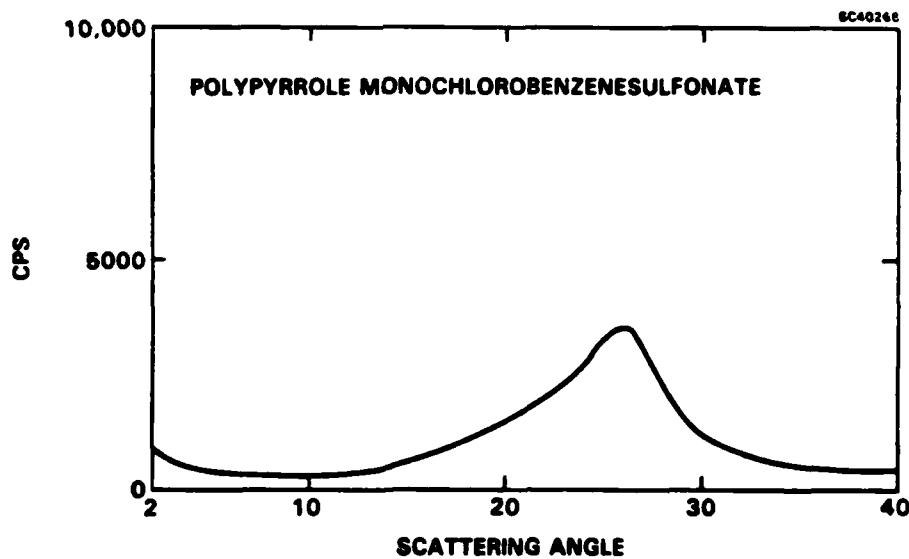


Fig. 11 Polypyrrole Monochlorobenzenesulfonate (MCBSH); 0.1M MCBSH; 0.1M  
pyrrole; ITO electrode;  $\sigma = 120 \Omega^{-1}\text{-cm}^{-1}$ .

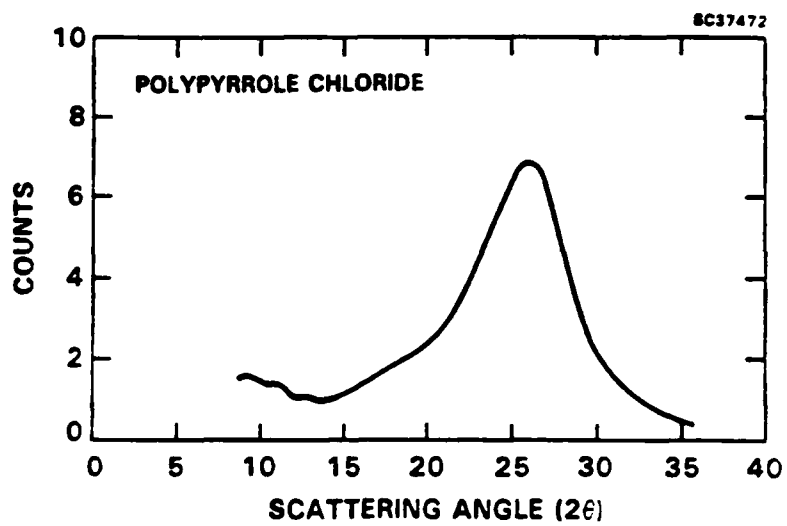


Fig. 12 Polypyrrole chloride, 0.3M HCl (water); 0.1M pyrrole; Au electrode,  $\sigma = 9.2 \Omega^{-1}\text{-cm}^{-1}$ .

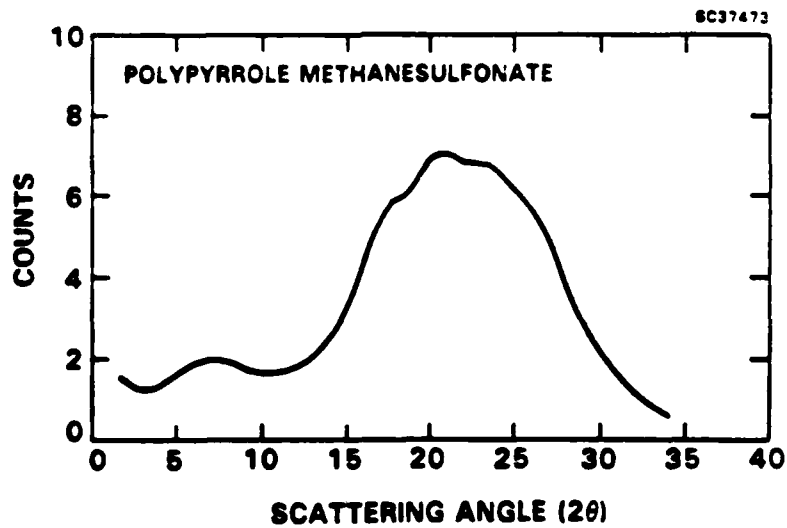


Fig. 13 Polypyrrole methane sulfonate (MES); 0.1M HMES; 0.1M pyrrole; Au electrode,  $\sigma = 2 \Omega^{-1}\text{-cm}^{-1}$ .

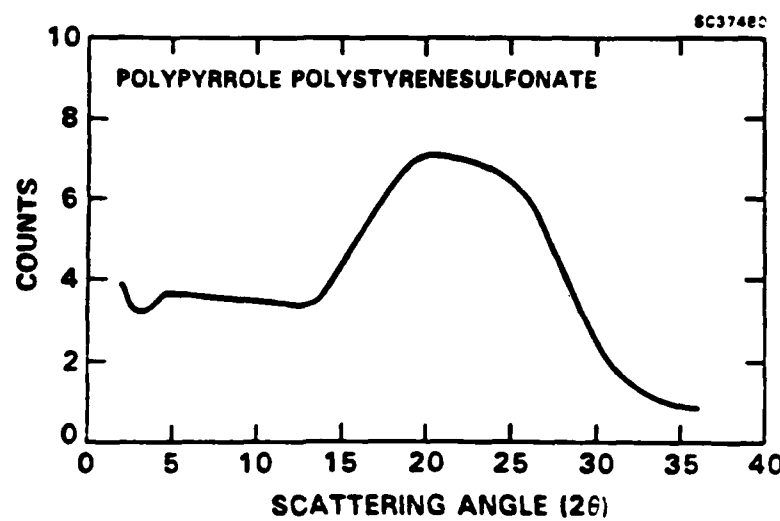


Fig. 14 Polypyrrole polystyrene sulfonate (PSSA); 0.1M PSSA; 0.1M pyrrole; pH - 1.9; Au electrode,  $\sigma = 8 \Omega^{-1}\text{-cm}^{-1}$ .

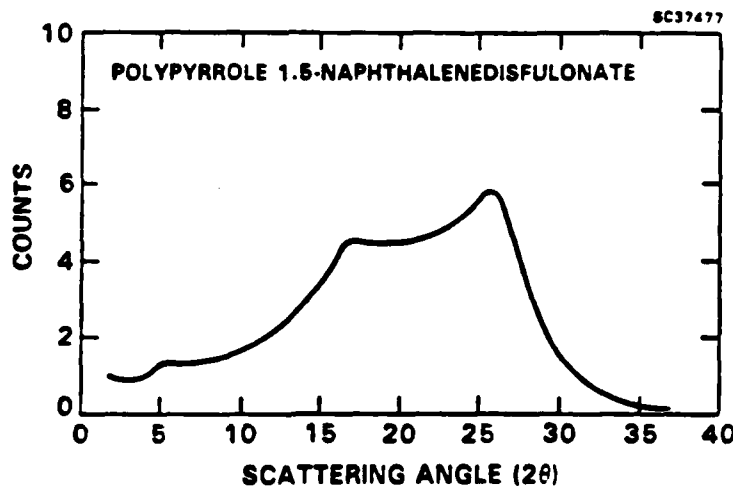


Fig. 15 Polypyrrole 1,5-NDS; 0.1M 1,5-NaNDS; 0.1M pyrrole; PG electrode,  $\sigma = 14 \Omega^{-1}\text{-cm}^{-1}$ .

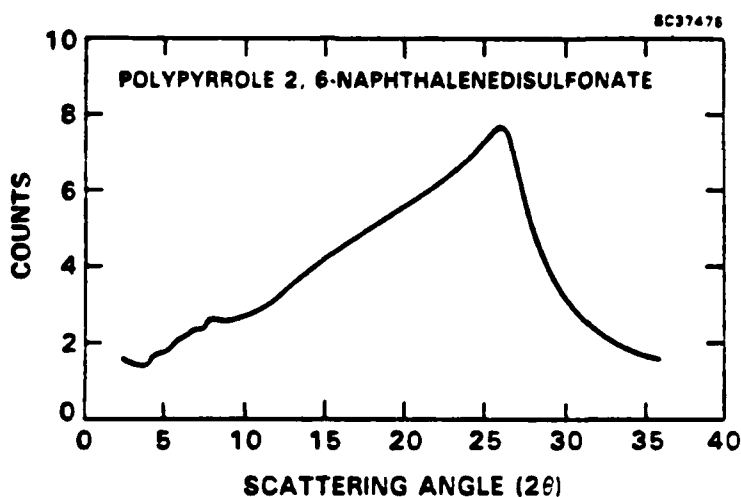


Fig. 16 Polypyrrole 2,6-naphthalene sulfonate (NDS); 0.1M Na 2,6NDS; 0.1M pyrrole; pH = 6.6; Au electrode,  $\sigma = 75 \Omega^{-1}\text{-cm}^{-1}$ .

The x-ray results obtained on the polypyrrole films are consistent with previous diffraction results presented by Wegner<sup>3</sup> on a series of polypyrrole "tensides." Wegner related the low angle peak in the x-ray diffraction pattern of these materials to the length of the alkyl chain of the dopant ion and postulated that the absence of higher order in these materials implies that the underlying structure of the polymer is very distorted, probably liquid like. The results obtained in the present work seem to confirm these statements. Evidently, the lack of long range order in this material causes the polymer to grow in an unoriented random fashion and probably indicates numerous chemical defects such as chain cross-links.

It has been stated that an organic polymer cannot be completely crystalline.<sup>2</sup> A crystalline polymer is always a semicrystalline substance comprising crystalline, paracrystalline and amorphous regions. Polypyrrole appears to consist of paracrystalline and amorphous regions. While detailed information on the crystal structure of polypyrrole is not available, the broad x-ray patterns can provide some information regarding the

d-spacings in the polymer lattice. Such information can be related to the structure of polypyrrole by considering hypothetical models for the structure of this polymer. A relevant model can be generated using bond length and bond angle data obtained from electron diffraction data<sup>5</sup> on the pyrrole monomer. The single bond lengths were found to be 1.44 Å, while the double bond lengths were found to be 1.35 Å. The interior angles of the monomer were found to be between 105° and 110°. Using these data, one can calculate relevant interatomic distances for a hypothetical planar pyrrole polymer. Shown in Fig. 17 is a segment of such a polymer, along with some calculated distances. As can be seen, the interatomic distance for alpha carbon atoms on adjacent monomer units is approximately 3.71 Å. This spacing corresponds to a Cu K<sub>α</sub> diffraction angle,  $2\theta$ , of approximately 24°. While many of the pyrrole polymers exhibit diffraction at this angle, the width of the diffraction peaks suggests that this spacing is not the exclusive contributor to the diffraction pattern.

SC37611

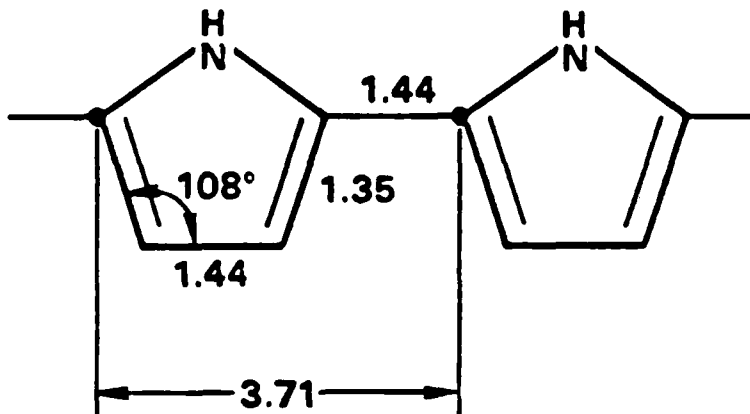


Fig. 17 Hypothetical polypyrrole segment.

Previous studies<sup>6</sup> on the crystal structure of cis-polyacetylene have shown that this polymer exists in an orthorhombic space group. The distance between chains along the b-axis was found to be 4.47 Å. While polypyrrole does not exhibit the degree of crys-

tallinity found in cis ( $\text{CH}_x$ ) and may not exist in the same space group, the distance between polymer chains in polypyrrole and cis ( $\text{CH}_x$ ) are probably similar. A distance of 4.47 $\text{\AA}$  corresponds to a  $2\theta$  value of 19.8°. As can be seen from Figs. 4-16, most of the polymers exhibit x-ray scattering around this angle. The x-ray patterns observed for the polypyrrole samples may be rationalized, then, on the basis of the superposition of two or three diffraction maxima corresponding to the multiple phases in the lattice. The broad nature of the x-ray scattering can be explained on the basis of the known disorder of the pyrrole polymers and the thermal vibrational broadening of the atoms in the polymer.

The data in Table 3 indicate that the dopant anions exert a significant influence on the microstructure of the electrodeposited polypyrrole. On the basis of the x-ray diffraction patterns produced by the polypyrrole films, it is possible to rank these polymers in terms of their relative degree of order. Thus, the film that contains the 1,2 ethanedisulfonate dianion gives rise to the lowest intensity x-ray scattering (Fig. 10) and appears to exhibit the lowest order. In contrast, the x-ray scattering curves obtained on the pyrrole polymers doped with tosylate, dodecylbenzenesulfonate, dodecylsulfate and the trichlorobenzenesulfonate anion, indicate that these polymers appear to exhibit the highest order.

While the x-ray scattering curves obtained on the polypyrrole films indicate that these materials are of low crystallographic order, a recent report describes a method for analyzing the domain size in amorphous polymers. Heeger and coworkers<sup>7</sup> analyzed the x-ray diffraction curves obtained on a closely related polymer, namely polyisothianaphthene (PITN), by use of the Scherrer equation (Eq. 1).

$$t = \frac{0.9 \lambda}{B \cos \theta} \quad (1)$$

They concluded, on the basis of the x-ray scattering curve, that the PITN material consists of crystallites approximately 20 $\text{\AA}$  in size. While it is realized that the Scheerer equation was derived for use in crystalline solids,<sup>8</sup> application of this relation to a series of closely related amorphous solids nevertheless yields qualitatively meaningful results. An analysis of our diffraction curves by use of the Scherrer relation has been carried out. The results, presented in Table 4, suggest that the polymers with the largest domain

**Table 4**  
**X-Ray Diffraction Data Used for Coherence Length Calculations**

Dopant-Ion	Peak Maxima (°)	PWHH	Coherence Length
Monochlorobenzenesulfonate	26.1	7.7	21.83
Trichlorobenzenesulfonate	26.0	5.5	30.14
Dodecylsulfate	20.5	7.3	22.84
Dodecylbenzenesulfonate	22.5	10.8	15.32
Chloride	26.0	7.2	23.39
Polystyrenesulfonate	21.0	15	10.93
Tosylate	21.25	12.6	13.06

sizes contain the larger aromatic sulfonate monoanions or long aliphatic chain sulfates. Of particular note is the relatively large coherence length, 30.94 Å, found in the trichlorobenzenesulfonate-doped polymer. This polymer appears to exhibit the greatest degree of order of all the doped pyrrole polymers prepared in this program.

The effect of the dopant ion upon the order or crystallinity of the polypyrrole films is quite significant. On the other hand, the deposition solvent also appears to exert a smaller but noticeable effect upon the morphology of the polypyrrole films. In general, polypyrrole films deposited from aqueous solutions are of lower quality and give rise to broader diffraction patterns than the corresponding films deposited from acetonitrile. In some instances, the general shape and peak multiplicity of the x-ray scattering curves are different. This effect is seen upon examination of the x-ray scattering curves obtained on films of polypyrrole tosylate deposited from water and acetonitrile. As can be seen from Figs. 8 and 9, both polymer films give rise to broad x-ray scattering patterns, however, the higher angle scattering pattern shown in Fig. 8 (aqueous deposition) clearly appears to be the superposition of two diffraction peaks while the corresponding scattering pattern shown in Fig. 9 (acetonitrile deposition) only appears as a single peak. The peak multiplicity obviously implies different crystallographic orientations of the polymer chains or multiple phases but at this point it is not possible to assign these phases.

To a first approximation, the degree of order present in the polypyrrole-dopant complexes also influences the conductivity of the polymers as well as their other physical properties such as film quality or tensile strength. As seen from Table 1, the most highly conducting polymers were the tosylate, monochlorobenzenesulfonate and trichlorobenzenesulfonate-doped materials. These polymers also exhibit the greatest degree of order as judged by the x-ray scattering curves. On the other hand, the nearly equally ordered chloride and dodecylsulfate-doped polymers exhibit an order of magnitude lower conductivity levels. This may be attributable to the fact that the latter set of polymers were deposited from water while the former set were deposited from acetonitrile. The film quality also appeared to correlate well with the degree of polymer order and conductivity levels. The toughest and most flexible films were the tosylate, monochlorobenzenesulfonate and trichlorobenzenesulfonate polymers deposited from acetonitrile while the most brittle and least conductive films appeared almost amorphous by x-ray.

The foregoing discussion strongly suggests that the physical properties of the electrodeposited polypyrrole films show a positive correlation with their degree of order. However, additional supporting evidence for polymer anisotropy obtained from other techniques would be of significance. A new voltammetric technique first developed under Rockwell IR&D appears to indicate the degree of order in thin polypyrrole films. A positive correlation of these voltammetric results with the x-ray scattering curves would be sufficient proof. In this method, the magnitude and sharpness of the first voltammetric reduction peak of a deposited film is recorded in a solvent containing only supporting electrolyte. Following from the concept that equivalent redox sites of the film would reduce at the same potential, a sharper reduction peak would denote a smaller distribution of redox sites, and hence greater order. The first cathodic process involves dopant anion expulsion from the film and subsequent voltage cycles do not reproduce the initial voltammetric peaks. Figure 18 displays representative current-voltage curves for an as-deposited polypyrrole thin film. The voltammetric response features of the first cathodic scan of as-deposited (from water) thin films are presented in Table 5. Note that the same amount of charge was used to deposit all of these films. Terms characterizing the "sharpness" of these peaks are defined in Fig. 18. The data show that the most intense and narrow reduction peaks and hence the highest degrees of order are associated

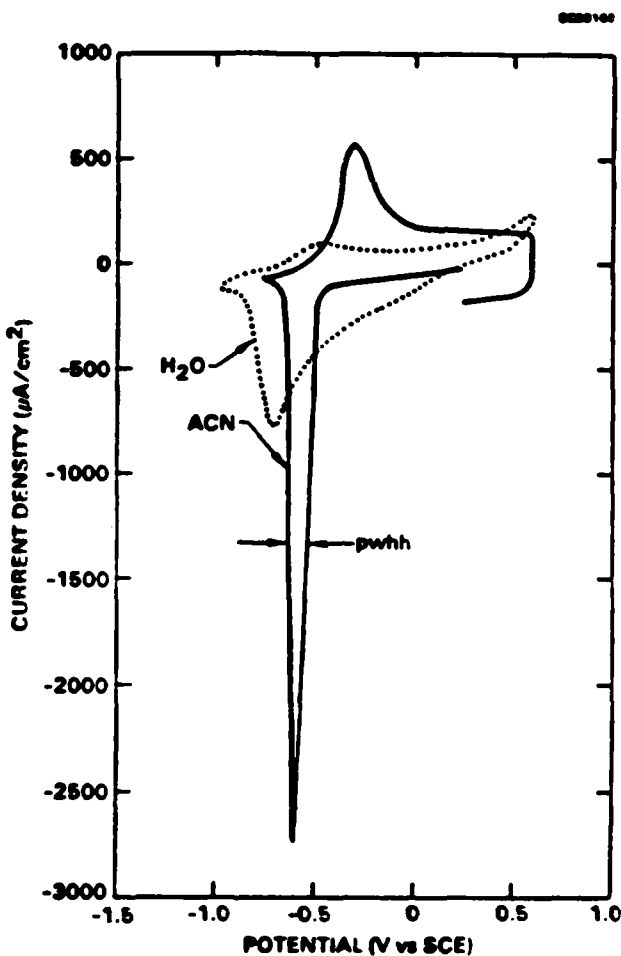


Fig. 18 First reduction cycle of as-deposited polypyrrole tosylate thin films, evaluated in deoxygenated 0.1M aqueous sodium tosylate (dotted curve) and in 0.1M tetraethylammonium tetrafluoroborate in acetonitrile (solid curve), scan rate 50 mV/s, film thickness corresponds to 40 mC/cm<sup>2</sup> of charged passed, pwth = peak width at half height.

with two dopant types: (1) benzene aromatics and (2) long aliphatic chain dopants. Films displaying intermediate peak width/height values are produced by the larger naphthalenesulfonate monoanions and dianions. The poorest quality films are formed with smaller organic and inorganic anions. From Table 5, the standout anions for conferring order in polypyrrole films are the tosylate, dodecylbenzenesulfonate, p-chlorobenzene-sulfonate and trichlorobenzenesulfonate. The size and shape of the stand-out anions

apparently fits well within the lattice of the polypyrrole and allows the polymer to grow in a more uniform and ordered structure. These results are corroborated by the x-ray scattering results discussed previously and attest to the voltammetric response technique as being a simple and reliable method for the rapid screening of structural order in polypyrrole-dopant systems.

#### 1.4.2 Transmission Electron Microscopy

An alternative method for the determination of the degree of crystallinity of a material is Transmission Electron Microscopy (TEM). The use of the electron microscope allows one to examine the material under very high magnification and for sufficiently crystalline material, allows determination of the lattice dimensions and symmetry. This technique is ordinarily performed on very thin, nearly transparent material deposited on standard minigrids. The successful use of the electron microscope relies on exacting sample preparation techniques. Thick samples do not transmit the diffracted electrons. Sample preparation techniques that have been previously used include particle suspension depositions and microtoming. Under this contract, we have investigated two methods for TEM sample preparation: (1) direct electrodeposition of the polymer on the TEM grid and (2) application of polymer particles onto the TEM grid. The electrodeposition technique provided the best samples for TEM observation of the electrodeposited materials while the second method was most applicable to the chemically prepared polypyrrole polymers described in a following section.

Samples of polypyrrole suitable for TEM measurements were prepared by directly depositing the conductive polymer onto the gold minigrid. This was accomplished by immersing the grid, gripped by a gold-plated alligator clip, into the monomer/electrolyte solution and then applying a constant anodic current of about  $1 \text{ mA/cm}^2$  to the grid. The deposition was terminated after periodic inspection of the grid revealed sufficient polymer growth within the grids. It should be noted that the optimal conditions for TEM sample preparation were not those used for thick, free-standing film preparation but rather those that promoted fibril or nodular-type growth in the grid spacings (see Table 2). Displayed in Figs. 19 and 20 are magnified views of a sample of polypyrrole tosylate deposited onto the gold minigrid. As can be seen from

**Table 5**  
**Effect of Various Anions on the First Reduction Peak of As-Deposited Polypyrrole Films from Aqueous Electrolytes**

Dopant Anion	Evaluation Solvent	Scan Rate (mV/s)	$I_{pc}$ ( $\mu\text{A}/\text{cm}^2$ )	$E_{pc}$ (mV vs SCE)	$q_c/q_d$	pwhh (mV)	m.
Tosylate	ACN	50	1430	-770	0.156	50	1
	$\text{H}_2\text{O}$	50	345	-700	0.175	300	1
p-CIBS	ACN	50	1250	-750	0.148	120	1
$\text{Cl}_3\text{BS}$	ACN	50	1040	-750	0.142	80	1
	$\text{H}_2\text{O}$	50	800	-800	0.164	160	1
$\text{C}_{12}\text{BS}$	ACN	50	830	-820	0.151	180	1
	$\text{H}_2\text{O}$	50	990	-690	0.167	120	1
$\text{C}_{12}\text{OSO}_3^-$	$\text{H}_2\text{O}$	50	525	-590	0.171	210	2
2-NS	$\text{H}_2\text{O}$	100	650	-580	0.182	430	2
4,4'-BPDS	ACN	50	665	-1030	0.166	350	1
	$\text{H}_2\text{O}$	50	265	-420	0.189	475	
2,6-NDS	ACN	50	720	-980	0.141	260	2
1,5-NDS	ACN	50	450	-970	0.159	500	1
	$\text{H}_2\text{O}$	100	560	-560	0.174	470	3
PSS	ACN	50	380	-910	0.162	285	1
	$\text{H}_2\text{O}$	50	273	-650	0.176	470	2
$\text{CH}_3\text{SO}_3^-$	$\text{H}_2\text{O}$	50	190	-750	0.142	640	3
$\text{HSO}_4^-$	$\text{H}_2\text{O}$	50	220	-510	0.127	500	2
$\text{Cl}^-$	$\text{H}_2\text{O}$	50	200	-740	0.144	750	2

ACN evaluation solvent was 0.1M tetraethylammonium tetrafluoroborate; aqueous evaluation solvent was 0.1M sodium tosylate.  $I_{pc}$  = cathodic peak current.  $E_{pc}$  = peak potential of cathodic wave.  $q_c/q_d$  = ratio of integrated cathodic charge on first scan to total charge to produce film (18.1 mC). pwhh = peak width at half-height. m = multiplicity of cathodic wave. Chemical terms: p-CIBS = p-chlorobenzenesulfonate;  $\text{Cl}_3\text{BS}$  = 2,4,5-trichlorobenzenesulfonate;  $\text{C}_{12}\text{BS}$  = dodecylbenzenesulfonate;  $\text{C}_{12}\text{SO}_4^-$  = dodecylsulfate; 2-NS = 2-naphthalenesulfonate; 4,4'-BPDS = 4,4'-biphenyldisulfonate; 2,6-NDS = 2,6-naphthalenedisulfonate; 1,5-NDS = 1,5-naphthalenedisulfonate; PSS = polystyrenesulfonate.

SC37857

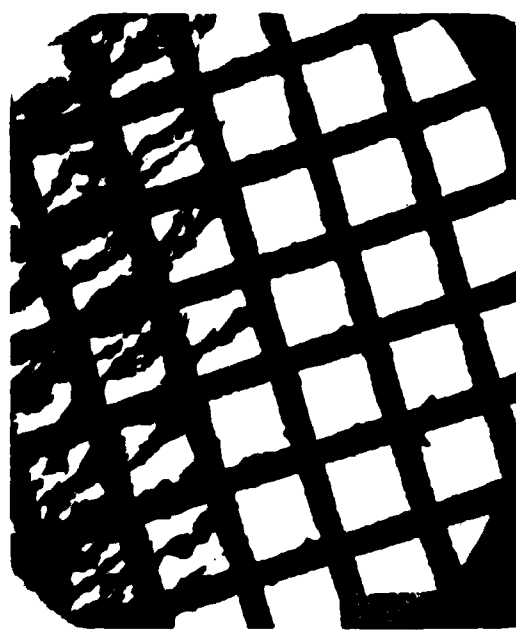


Fig. 19 TEM photograph of electrodeposited polypyrrole tosylate.

SC37858

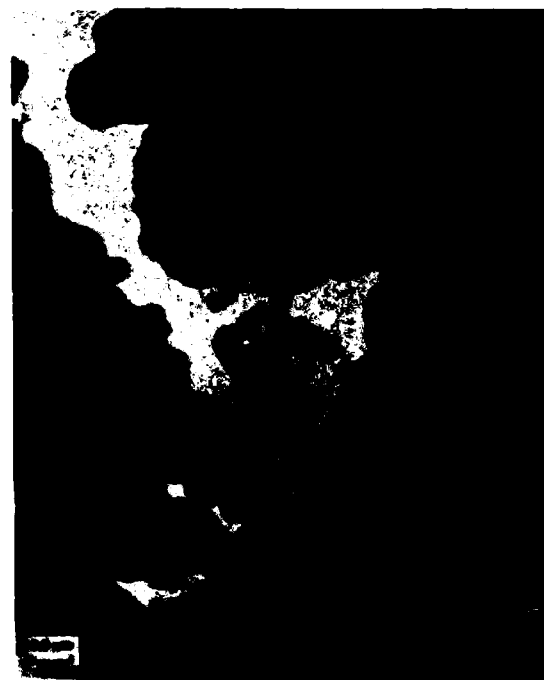


Fig. 20 TEM photograph of electrodeposited polypyrrole tosylate.

these photographs, there are numerous polymer fibers growing across the grid openings. Examination of the thinnest portions of these fibers by electron diffraction does not reveal any diffraction evidence of crystallinity. A thin film is observed to stretch across the grid openings. This film gives rise to the electron diffraction pattern observed in Fig. 21. From these photographs, it is seen that the polymer apparently grows in more than one morphological phase and that crystallinity is observed in one phase. The relationship of the crystalline phase to the amorphous phase is not known but it is worth noting that the crystalline phase corresponded to the thinnest portion of the polymer film. This observation may suggest that the nascent polymer grows in a semicrystalline morphology while the bulk polymer subsequently develops into an amorphous phase.

Other samples of doped polypyrrole have also been examined by TEM. For example, TEM photographs of two separate regions of polypyrrole dodecylsulfate deposited from aqueous solution are shown in Figs. 22 and 24 and the electron diffraction photographs produced by the thin polymer deposits are illustrated in Figs 23 and 25. As was the case for the tosylate-doped polymer, the dodecylsulfate-doped polymer appears to grow in more than one morphological phase; the crystalline phase occurring in the thinnest, least-developed portion of the sample. While limited amounts of crystallinity were detected in the tosylate and dodecylsulfate-doped polymers, no evidence of crystallinity could be detected in TEM samples of polypyrrole dodecylbenzenesulfonate (Figs. 26 and 27) that were prepared under several sets of experimental conditions.

The polypyrrole-chlorobenzenesulfonates were also examined by TEM. These derivatives appeared to exhibit the greatest degree of order according to the x-ray diffraction patterns. As seen from the TEM photographs (Fig. 28-30) the monochlorobenzenesulfonate-doped material exhibited some crystallinity in the thinnest regions of the sample. In contrast, a deposit of the pentachlorobenzenesulfonate-doped polymer that grew in a spheroidal morphology, did exhibit any evidence of crystallinity (Figs. 31 and 32). TEM photographs of the trichlorobenzenesulfonate-doped material (Fig. 33 and 34) show that this polymer also contains crystalline components. Thus, these dopant anions appear to confer a greater degree of order to the structure of the polypyrrole than others that were examined in this work. This ability to order polypyrrole may be due to several features of these anions. First, the bulky size of the chloride substituents may

SC40378



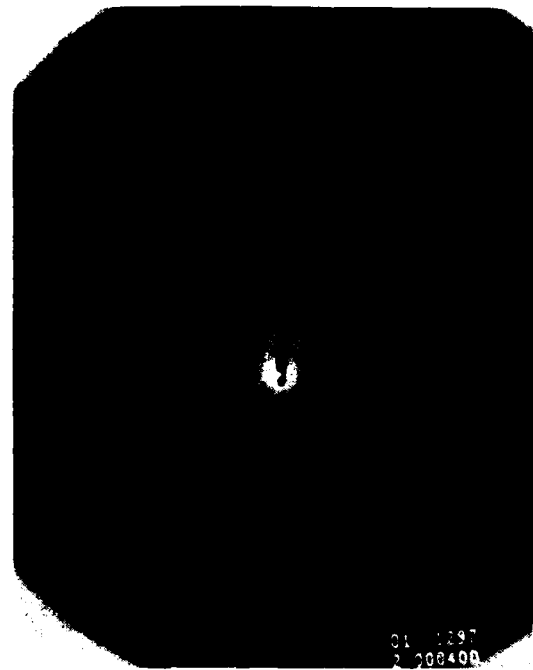
Fig. 21 Diffraction pattern from discrete particles on continuous film.

SC37561



Fig. 22 TEM photograph of electrodeposited polypyrrole DDS.

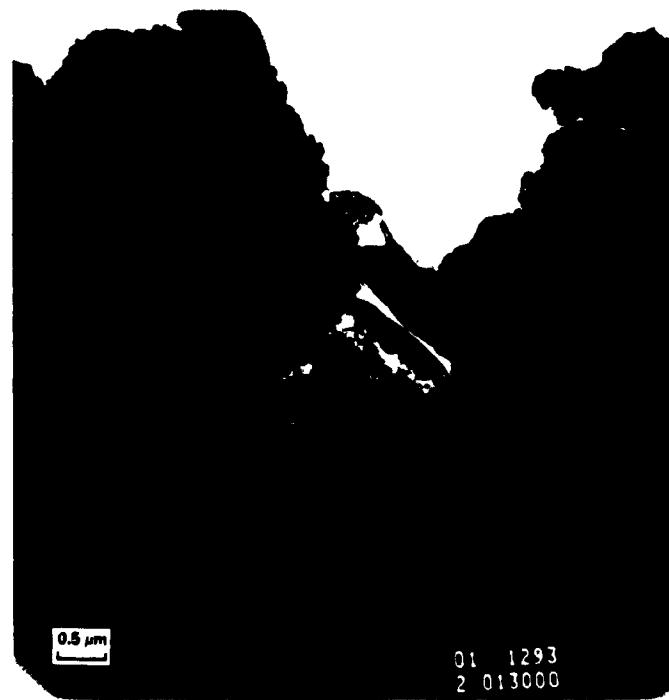
SC37662



01 1297  
2 013000

Fig. 23 TEM photograph of electrodeposited polypyrrole DDS.

SC37560

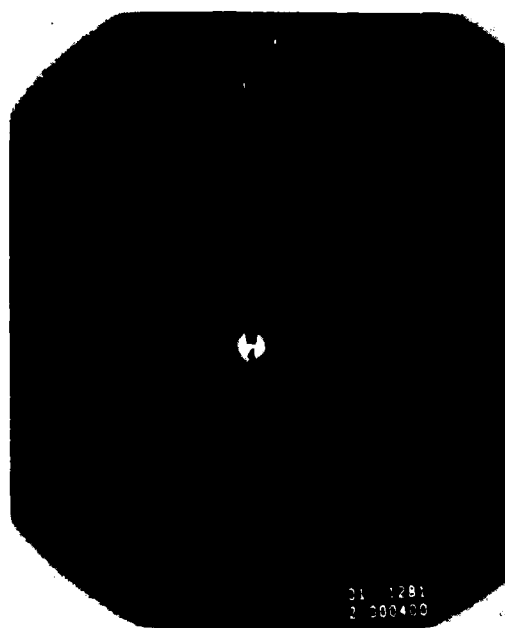


0.5 μm

01 1293  
2 013000

Fig. 24 TEM photograph of electrodeposited polypyrrole DDS.

SC37559



01 1281  
2 000400

Fig. 25 Electron diffraction pattern electrodeposited polypyrrole DDS.

SC37564

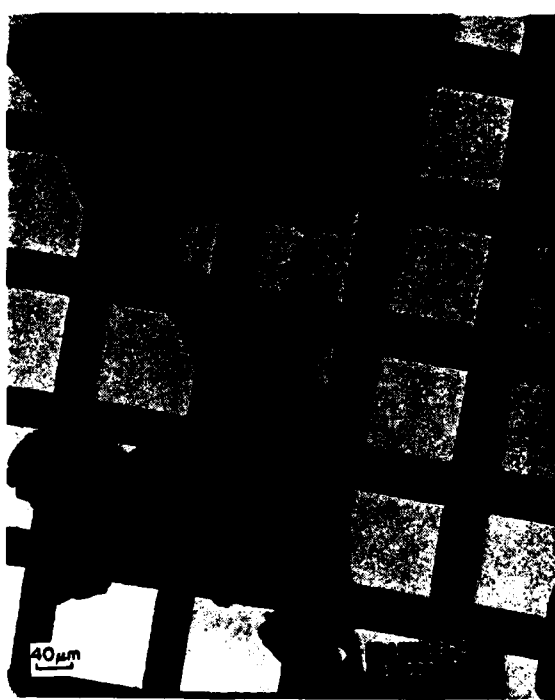


Fig. 26 TEM photograph of electrodeposited polypyrrole DDS.

NADC-87092-60

SC37563

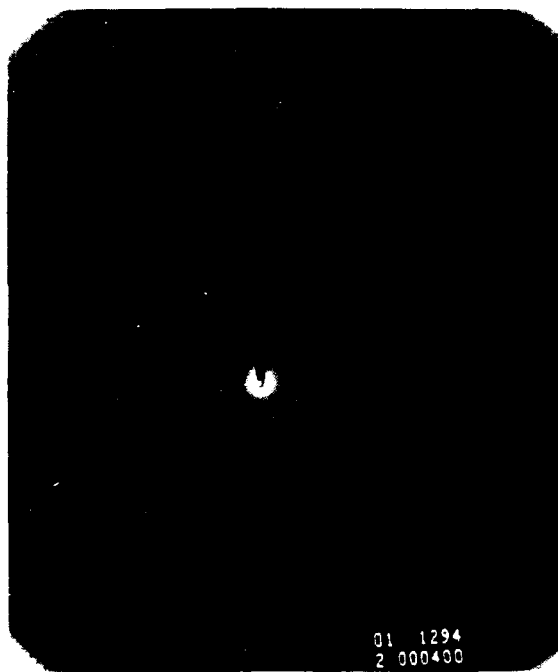


Fig. 27 Electron diffraction pattern of electrodeposited polypyrrole DDBS.

SC40379



Fig. 28 TEM photograph of a thin film of polypyrrole MCBS with crystalline grains.

SC40380

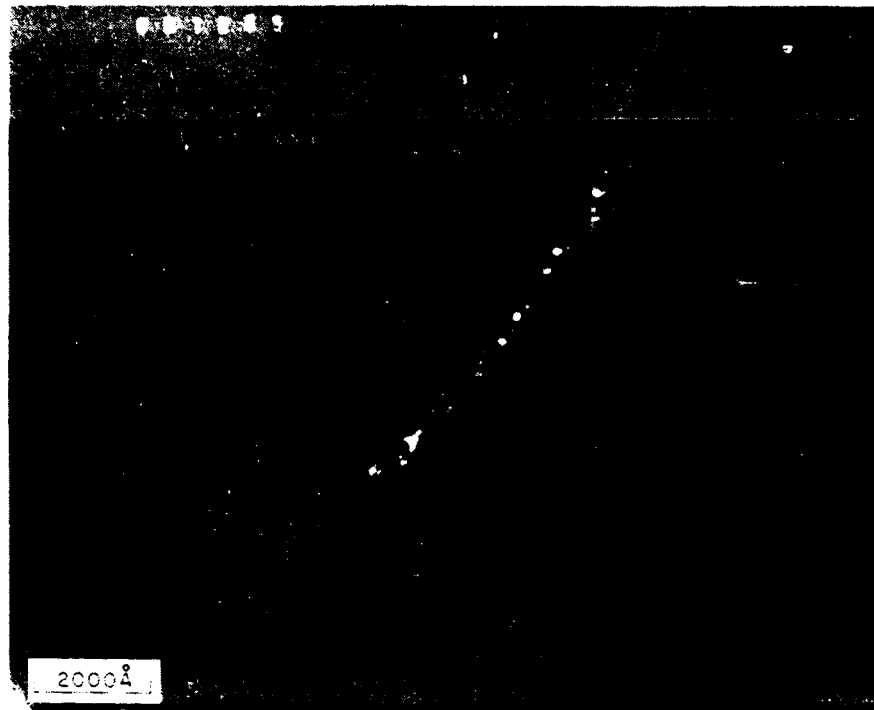


Fig. 29 Dark field TEM photograph of polypyrrole MCBS showing crystalline grains.

SC40381

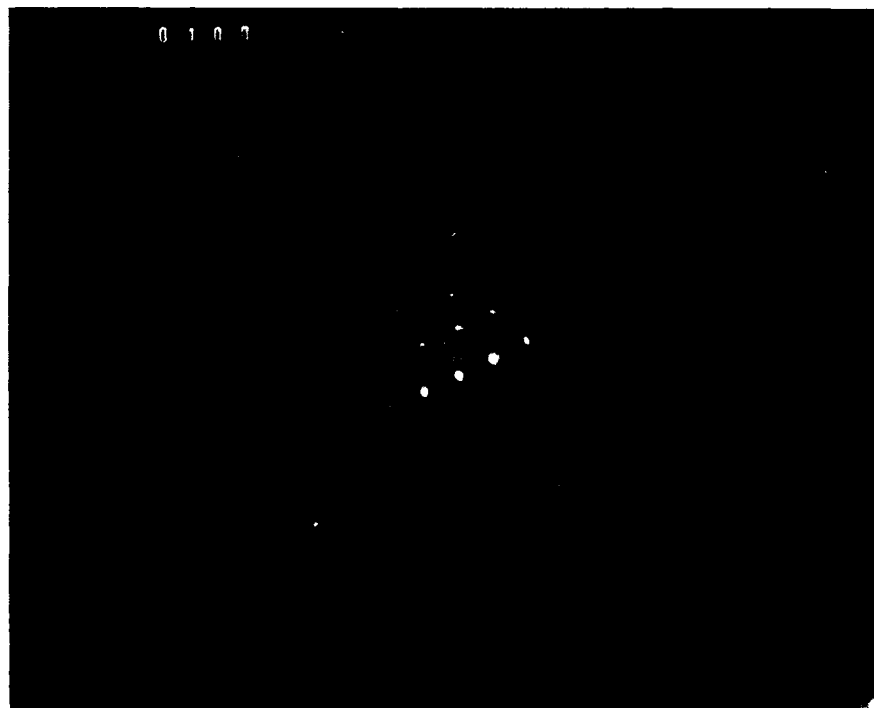


Fig. 30 Diffraction pattern from thin film of polypyrrole MCBS.

SC40382



Fig. 31 TEM photograph of polypyrrole PCBS; film is agglomeration of spheroids.

SC40383



Fig. 32 Diffraction pattern from spheroids of polypyrrole PCBS.

NADC-87092-60

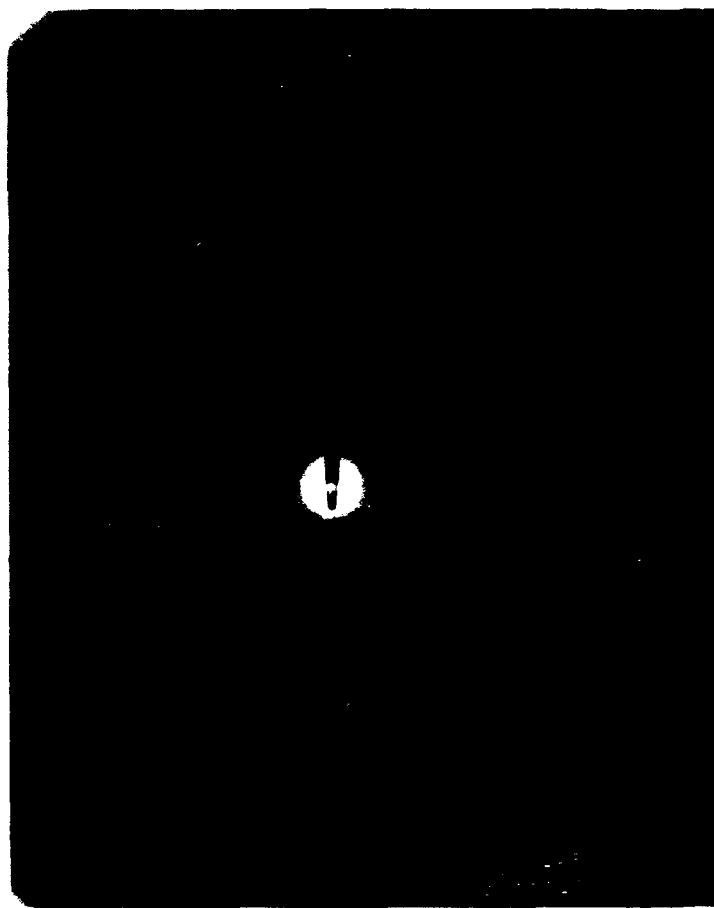
SC40384



Fig. 33 TEM photograph of polypyrrole TCBS.

NADC-87092-60

SC40385



**Fig. 34 Diffraction pattern from fiber of polypyrrole TCBS.**

attenuate side reactions during the formation of the polymer film and therefore lead to a more uniform and ordered structure. Secondly, weak Van der Waals attractions between chloride atoms may serve to provide additional lattice interactions and lead to a more ordered structure.

### 1.5 Conclusions

The effect of the incorporated dopant ion upon the morphology of polypyrrole was investigated by use of x-ray diffraction and transmission electron microscopy. While polypyrrole is found to be largely amorphous, some polymer-dopant combinations are found to be more ordered than others. In general, the use of either benzene aromatic sulfonate dopants or long chain aliphatic sulfates produces polypyrroles exhibiting the greatest degree of order. The polymers containing the naphthalene sulfonates and disulfonates do not exhibit as much order. The degree of order was correlated with the conductivity and mechanical properties of the polymer films. TEM characterization of the polymers confirmed that the polymers that exhibited the greatest degree of order as judged by the x-ray scattering curves, also contained detectable crystalline components. Further, TEM measurements indicated that very thin undeveloped polymer samples contained a greater degree of crystallinity than thicker, more developed polymers.

A recently developed voltammetric technique for the evaluation of order in thin films of polypyrrole-dopant was related to the x-ray diffraction patterns. The sharpness of the first reduction peak of the as-synthesized polypyrrole films was correlated with the order of the polymer. Thus, a simple and rapid technique is now available for assessing order in polypyrrole-dopant combinations.

## 2.0 CHEMICALLY DEPOSITED POLYPYRROLE

Most studies on polypyrrole have focussed on electrochemically deposited materials. Recently, however, a chemical method to prepare electrically conducting polypyrrole has been described.<sup>9</sup> This method relies on the simultaneous oxidation and polymerization of pyrrole monomer with ferric salts of organic sulfonates. As these materials may be valuable alternatives to the electrodeposited polymers, it was of interest to characterize them by TEM and x-ray diffraction.

Samples of chemically prepared polypyrrole suitable for TEM measurements were prepared by a two-step procedure. Thus, a solution of a ferric sulfonate was placed onto a glass slide, leaving a thin film of the oxidant on the slide. The glass slide was placed into a closed jar containing a small amount of pyrrole monomer. As the pyrrole vapors diffused onto the glass slide, a thin black polymer coating developed on the slide. The polymer-coated slide was removed from the jar and carefully rinsed with methanol to remove the remaining oxidant and by-products. A thin, nearly transparent portion of the deposit was transferred to the TEM grid. Representative TEM micrographs of the chemically prepared triflate polymer are shown in Figs. 35-37. As seen from these figures, the thin film that is stretched across the openings of the grid is composed of many individual hexagonal or octagonal particles about 1000Å in diameter but as seen in Fig. 37 these particles do not produce any diffraction reflections. These particles probably arise from the amorphous polymerization of the monomer on the surface of the individual crystallites of the ferric salt, the size of the particle related to the quantity of ferric ion in the crystallites. Ferric tosylate and ferric ethylbenzenesulfonate produce similar polypyrrole deposits.

The lack of any detectable crystallinity in the chemically prepared polypyrrole powders as compared to the electrodeposited materials suggests that the structures and compositions of these two types of materials are not the same. Analytical results previously obtained on the ferric ion derived polypyroles indicate that substantial quantities of oxygen are incorporated in these polymers. In the case of the electrodeposited materials, the applied potential may serve to partially align the ionic conducting polymer which can result in a pseudo-ordered material. The mechanism for

SC37566

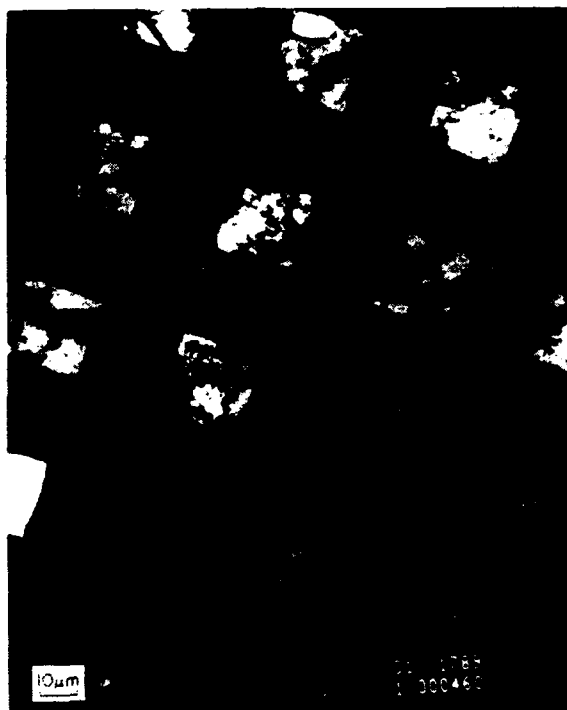


Fig. 35 TEM photograph of chemically deposited polypyrrole triflate.

SC37567



Fig. 36 TEM photographs of chemically deposited polypyrrole triflate.



Fig. 37 TEM photograph of chemically deposited polypyrrole triflate.

the formation of the chemically prepared polymers on the other hand is quite different. Polymer formation is influenced by the random diffusion of the oxidant and monomer. In the absence of an applied electric field, the resultant polymers adopt a nearly amorphous microstructure. The failure to detect crystallinity or order in the TEM images or in the x-ray diffraction curves of the powders is evidently a reflection of the amorphous nature of the chemically prepared polymers.

### 3.0 POLY-3-METHYLTHIOPHENE

#### 3.1 Introduction

As discussed in the previous sections, polypyrrole is a material of low crystallinity and is largely amorphous. Possible reasons for the low crystallinity of this polymer can include structural defects such as chain cross-links, beta-coupling of monomer units and the presence of pyrrolidinone end groups. These types of polymer defects probably arise because of the manifold of reaction pathways available to the intermediates involved in the polymerization of pyrrole monomer. This supposition suggests that circumvention of the side-reactions mentioned above may lead to a more uniform and possibly to a more crystalline polymer. A possible means of blocking some of the side reactions would be to introduce beta substituents onto the hetero-aromatic monomer. While 3-substituted pyrroles are not readily available, the iso-electronic 3-substituted methylthiophene monomer is available and has already been electro-polymerized.<sup>10</sup> In view of our efforts on the solid state characterization of polypyrrole, it was of interest to prepare doped poly-3-methylthiophene and examine this polymer by diffraction techniques.

#### 3.2 Experimental

Poly-3-methylthiophene films were deposited at constant current from a three electrode cell. The working electrode was either indium-tin oxide conducting glass or a gold-plated copper sheet. The counter electrode was a cylindrical platinum mesh electrode. The reference electrode was silver/silver nitrate/tetraethylammonium tetra-fluoroborate/ACN. The electrolytes were used as free acids at 0.1 M concentrations while monomer concentrations were 0.1-0.2 M. Under these conditions, constant deposition currents of  $6 \text{ mA/cm}^2$  produced voltages of 4.5 to 5.0 V. The best films were obtained using redistilled propylene carbonate. As-synthesized films were first soaked in propylene carbonate and then in methylene chloride and dried under a stream of nitrogen.

X-ray diffraction and TEM measurements were performed as described in the preceding section.

### 3.3 Results and Discussion

#### 3.3.1 Poly-3-methylthiophene Film Synthesis

Poly-3-methylthiophene can be prepared by electrodeposition techniques similar to those used for the preparation of polypyrrole. Usually this polymer is deposited from dry, non-aqueous solvents such as acetonitrile or propylene carbonate in the presence of typical electrolytes such as tetraethylammonium perchlorate or tetrabutylammonium triflate. The conductivities of the electrodeposited poly-3-methylthiophene films prepared in this work range from 1 to 80 mho/cm, although several groups have reported synthesizing this film with conductivities in excess of 200 mho/cm.<sup>11</sup> While the doped polypyrrole films exhibit good environmental stability, the poly-3-methylthiophene films are sensitive to exposure to water and had to be stored in an inert atmosphere to prevent decay of electrical properties. The increased environmental stability of the pyrrole polymers compared to the 3-methylthiophene polymers is attributable to the lower oxidation potential of the pyrrole monomer compared to the thiophene monomer.

In contrast to the good mechanical properties exhibited by the polypyrrole films, the poly-3-methylthiophene films were usually brittle and quite fragile. Attempts to optimize the deposition conditions to produce better quality films did not dramatically alter the mechanical properties of the films. The best quality films are obtained from propylene carbonate at low temperatures in the range 0-5°C. The best electrolytes were tetrabutylammonium triflate, triflic acid or perfluorooctanesulfonic acid. Attempts to prepare poly-3-methylthiophene tosylate or dodecylbenzenesulfonate only resulted in the formation of soluble dark oligomers at the anode surface. Thus, two films of poly-3-methylthiophene containing the dopant ions triflate and perfluorooctanesulfonate were successfully prepared and characterized.

#### 3.3.2 X-Ray Diffraction

X-ray scattering curves were obtained on free-standing films of doped poly-3-methylthiophene. As these films could only be synthesized under very specific conditions, only three such polymer films were characterized by x-ray diffraction.

The triflate doped polymer gave rise to the x-ray diffraction pattern shown in Fig. 38. This scattering curve appears to contain three separate broad peaks at  $2\theta_{\text{max}} = 26^\circ, 16.5^\circ, 5^\circ$ . These diffraction angles correspond to d-spacings of 3.42, 5.37 and 17.67 Å, respectively. As in polypyrrole, the 3 to 5 Å spacings may roughly correspond to distances between monomer units along a chain or between chains. The x-ray diffraction pattern of this polymer is consistent with the data presented by Garnier et al for the same polymer.<sup>12</sup> Garnier assigned the highest angle diffraction peak to the spacings associated with the polymer backbone on the basis of the observation that the diffraction peak at  $17^\circ$  disappeared in the x-ray scattering curve of neutral poly-3-methylthiophene while the peak at  $26^\circ$  was still observed. Those workers did not report any diffraction peaks below  $10^\circ$ . The low angle diffraction peak observed in our work may correspond to spacings associated with the dopant ions or may represent the presence of a type of short-range structural order.

To determine the effect of temperature upon the microstructure of the polymer, a film of poly-3-methylthiophene triflate was deposited at  $-40^\circ\text{C}$  from a propylene carbonate solution containing monomer and triflic acid. The film produced under these conditions gave rise to the diffraction pattern displayed in Fig. 39. As can be seen from this figure, there are at least three peaks in this curve. The higher angle peak appears to be sharper and more intense in this curve, compared to the curve produced by the room-temperature-synthesized film. Based upon the assignments of the x-ray peaks proposed above, this sharper peak might indicate that more order exists in the polymer backbone in the material synthesized at  $-40^\circ\text{C}$ . The intermediate angle peak appears slightly shifted to a lower angle,  $15^\circ$ , and is broader and less intense. This may indicate that the dopant ions in the polymer are more randomly placed throughout the lattice. The lower angle peak in the x-ray diffraction pattern of the film synthesized at  $-40^\circ\text{C}$  appears as a doublet and is sharper than the corresponding peak in the diffraction pattern of the room temperature synthesized film. As mentioned, the lattice features that give rise to this low angle diffraction are not known. However, Garnier has proposed a helical structure for this polymer and calculated the coil diameter to be about 19 Å; a value in reasonable agreement with the observed d-spacing of 17.7 Å.

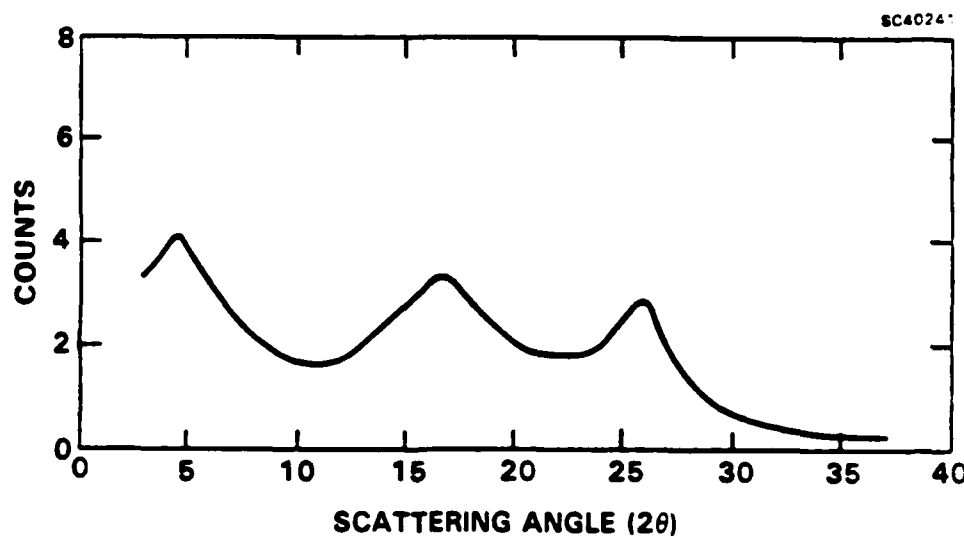


Fig. 38 X-ray diffraction pattern of poly(3-methylthiophene) trifluoromethane-sulfonate prepared at 0-5°C from propylene carbonate.

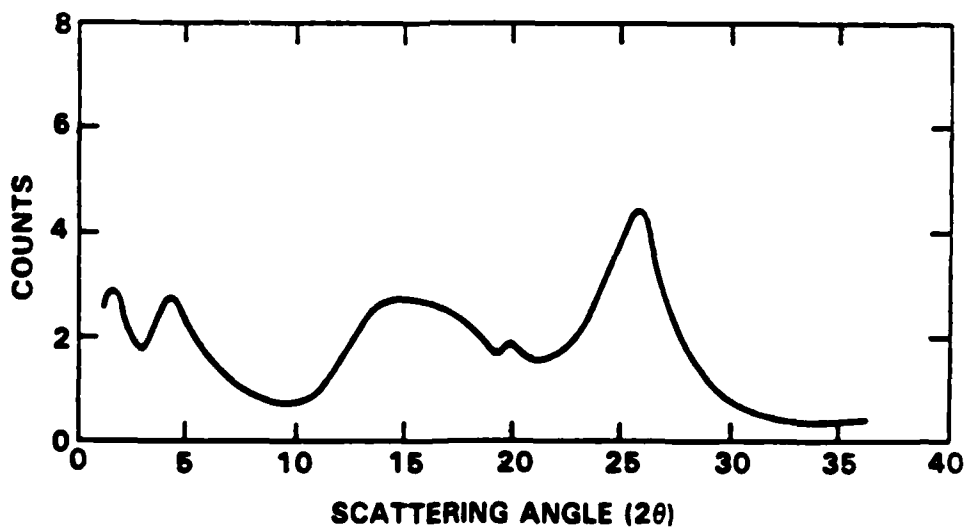


Fig. 39 X-ray diffraction pattern of poly(3-methylthiophene) trifluoromethane-sulfonate prepared at -40°C from propylene carbonate.

In contrast to the x-ray diffraction pattern produced by the film of poly-3-methylthiophene, the x-ray scattering curve shown in Fig. 40, of the perfluorooctanesulfonate-doped polymer film exhibits one broad peak,  $2\theta_{\text{max}} = 18^\circ$ , that probably consists of several overlapping peaks. The separated higher angle diffraction peak that was present in the scattering curve of the triflate polymer appears as a shoulder on the higher angle side of the main diffraction peak in the perfluorooctanesulfonate-doped polymer. The low angle diffraction of the perfluorooctanesulfonate-doped polymer appears significant and begins about  $7^\circ$ . However, due to instrumental limitations, it is not possible to determine the full extent of the low angle diffraction. This diffraction appears to continue down to very low angles. If we assume that the location of the diffraction maximum of the lower angle peak is around  $2^\circ$ , the corresponding lattice spacing is equal to about  $45\text{\AA}$ . The magnitude of this d-spacing suggests that a different type of ordering is present in this material as opposed to the triflate-doped polymer. From the diffraction pattern it is not possible to determine whether this spacing corresponds to distances along one polymer chain or to distances spanning a number of aligned polymer chains, but in any case, this polymer film appears to exhibit more order than is present in the polypyrrole films. This aspect of the morphology of poly-3-methylthiophene perfluorooctanesulfonate requires further investigation.

### 3.3.3 Transmission Electron Microscopy

Samples of doped poly-3-methylthiophene suitable for TEM were prepared by directly depositing the polymer onto the TEM grid as described for the polypyrrole samples. Figure 41 is a magnified photograph of a deposit of poly-3-methylthiophene triflate prepared using tetrabutylammonium triflate as the supporting electrolyte. As seen, this material develops with a fibrillar morphology. Higher magnification reveals (Fig. 42) a very thin polymer film that transmits electrons. This thin film is semi-crystalline as evidenced by the generated electron diffraction pattern (Fig. 43). As was the case for the polypyrrole films, crystallinity is only detected in the thin polymer regions. The thicker deposits are amorphous. Poly-3-methylthiophene triflate deposited from a solution containing triflic acid produces a polymer of comparable crystallinity. In comparison to the polypyrrole films, these materials are more crystalline and probably

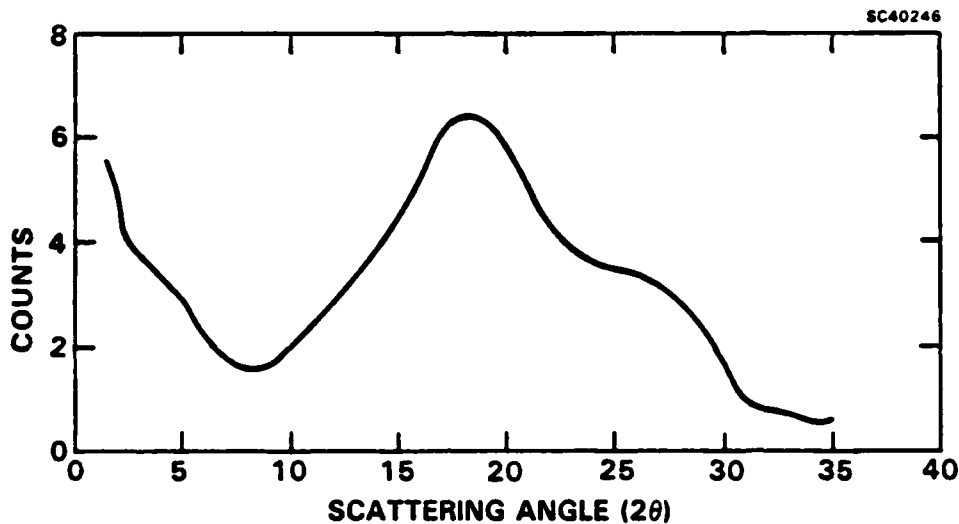


Fig. 40 X-ray diffraction pattern of poly(3-methylthiophene) perfluorooctylsulfonate prepared from propylene carbonate.

more ordered. Thus, the presence of the 3-methyl substituent on the aromatic ring apparently leads to a more uniform polymer that is able to adopt a semi-crystalline structure.

The perfluorooctanesulfonate-doped P3MT derivative was deposited onto a TEM grid from an acetonitrile solution containing monomer and the free acid. Figure 44 is a magnified photograph of this deposit. As can be seen, this material also grows in a fibrillar morphology. However, a portion of this deposit has grown in a thin continuous film. Examination of both regions of this deposit does not reveal any detectable crystallinity (Fig. 45).

While a tough, free-standing film of poly-3-methylthiophene hexafluorophosphate could not be obtained, it was possible to deposit this polymer-dopant material onto a TEM grid. As seen from Fig. 46, this material does not grow in a fibrillar

morphology and is not as crystalline as the triflate-doped polymer although hints of crystallinity are detected by electron diffraction.

### 3.3.4 Conclusions

The morphologies of several electrodeposited dopant anion-poly-3-methylthiophene combinations were examined by x-ray diffraction and TEM. These materials display more crystallinity than the polypyrrole materials but are still of relatively low crystallographic order. The polymer synthesis temperature was found to influence the degree of order of the polymer; lower temperature syntheses produced more ordered polymers. Because of the limited number of dopant-polymer combinations that are available with poly-3-methylthiophene, an extensive study of the role of dopant anions upon the morphology of poly-3-methylthiophene could not be carried out. The fact that poly-3-methylthiophene only forms with specific dopant ions, however, suggests that this polymer lattice is not as open or flexible as the polypyrrole lattice and probably indicates that the structure of the polymer is more uniform.

The x-ray diffraction pattern of perfluorooctanesulfonate-doped polymer exhibits significant low angle diffraction which may suggest that this dopant ion partially orders the polymer. Further investigations to clarify this point will be required.

SC35576

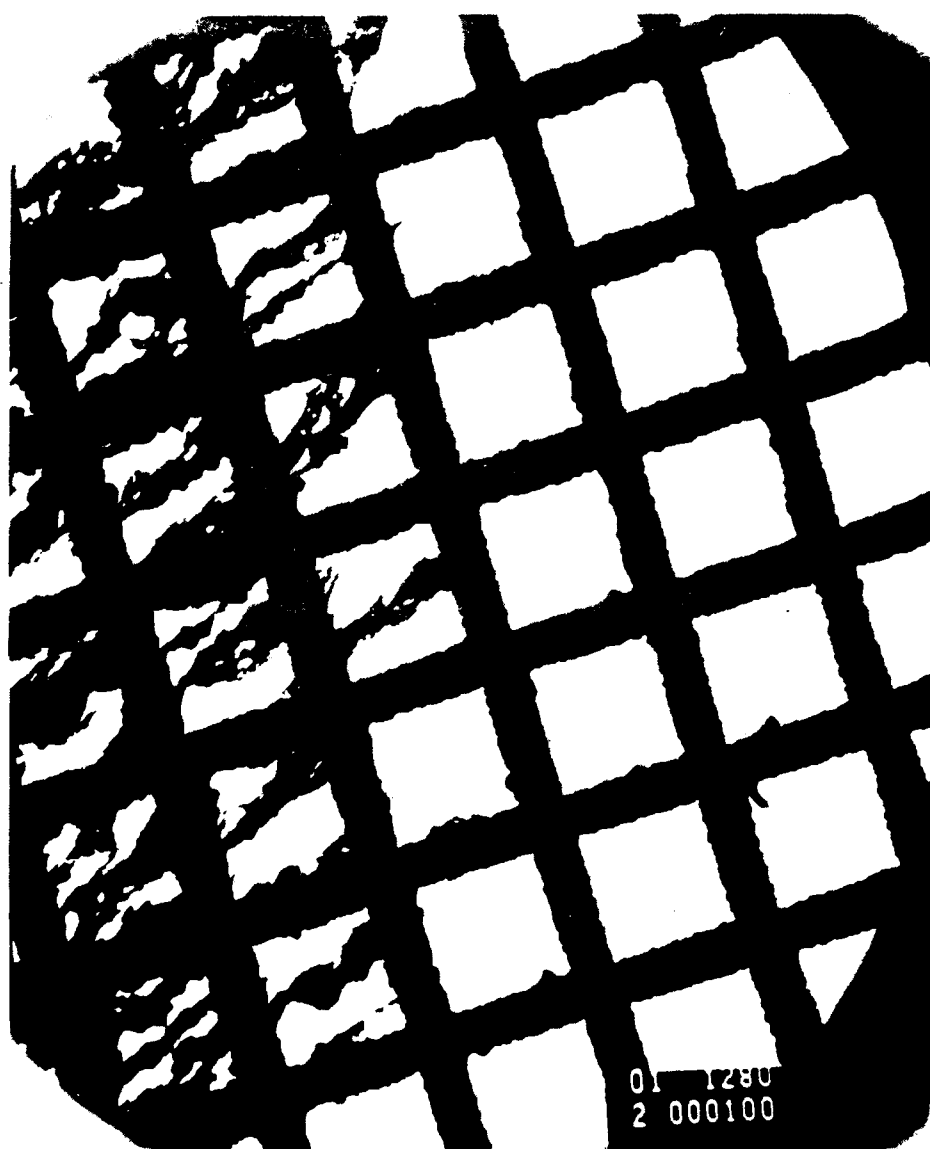


**Fig. 41** Magnified view of poly-3-methylthiophene triflate grown upon a TEM grid grown from 0.1M  $[\text{Bu}_4\text{N}] \text{CF}_3\text{SO}_3$  in acetonitrile.

NADC-87092-60

SC35580

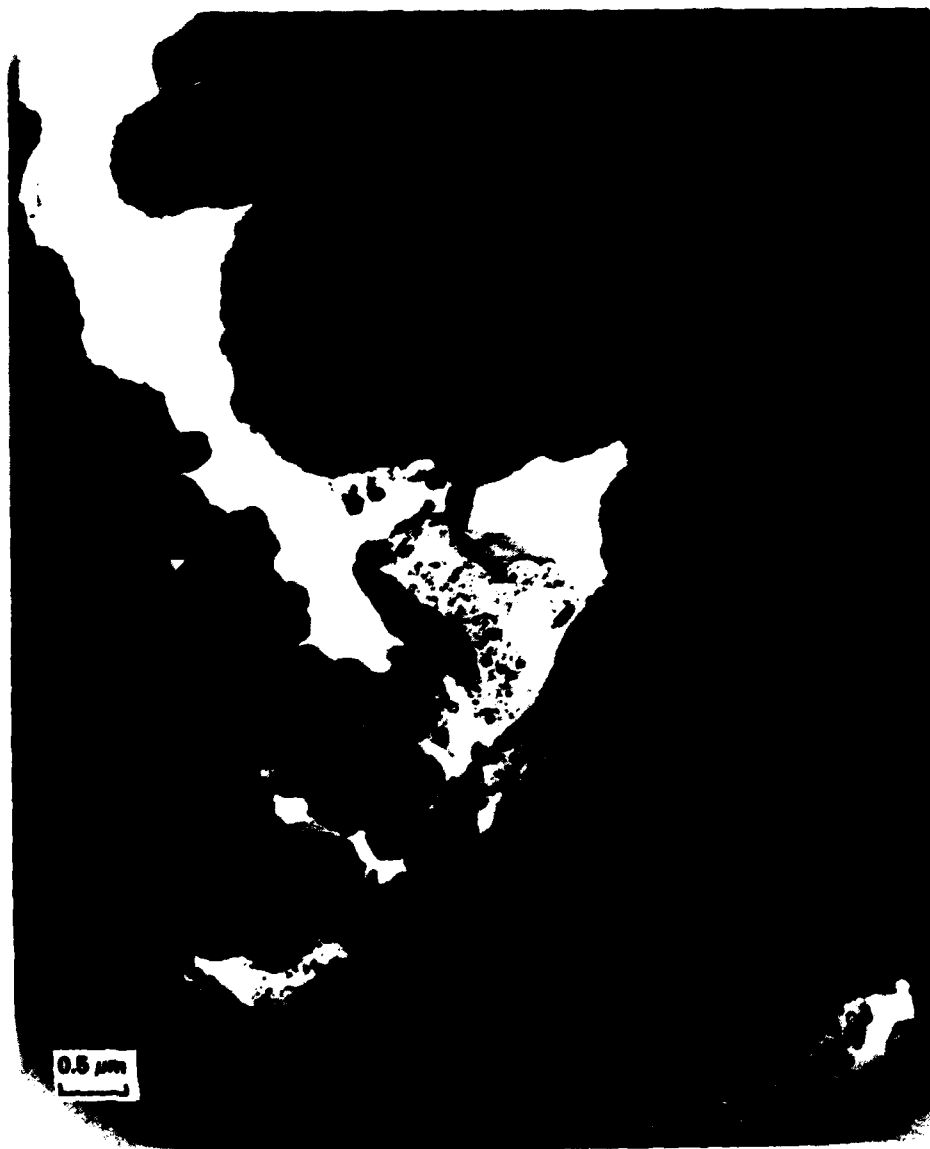
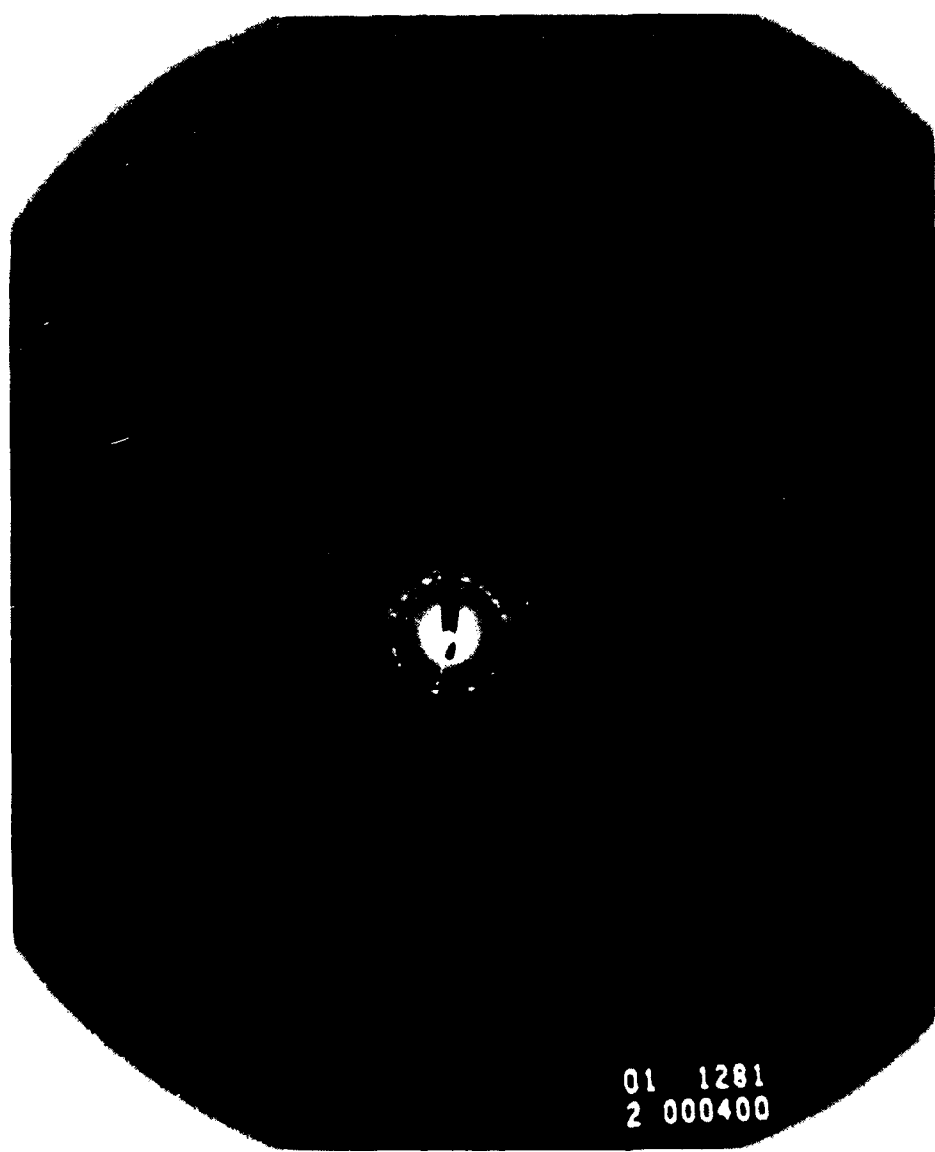


Fig. 42 Larger magnification of the polymer shown in previous figure.

NADC-87092-60

SC35579



01 1281  
2 000400

Fig. 43 Electron diffraction pattern produced by the polymer shown in previous figure.

SC35578

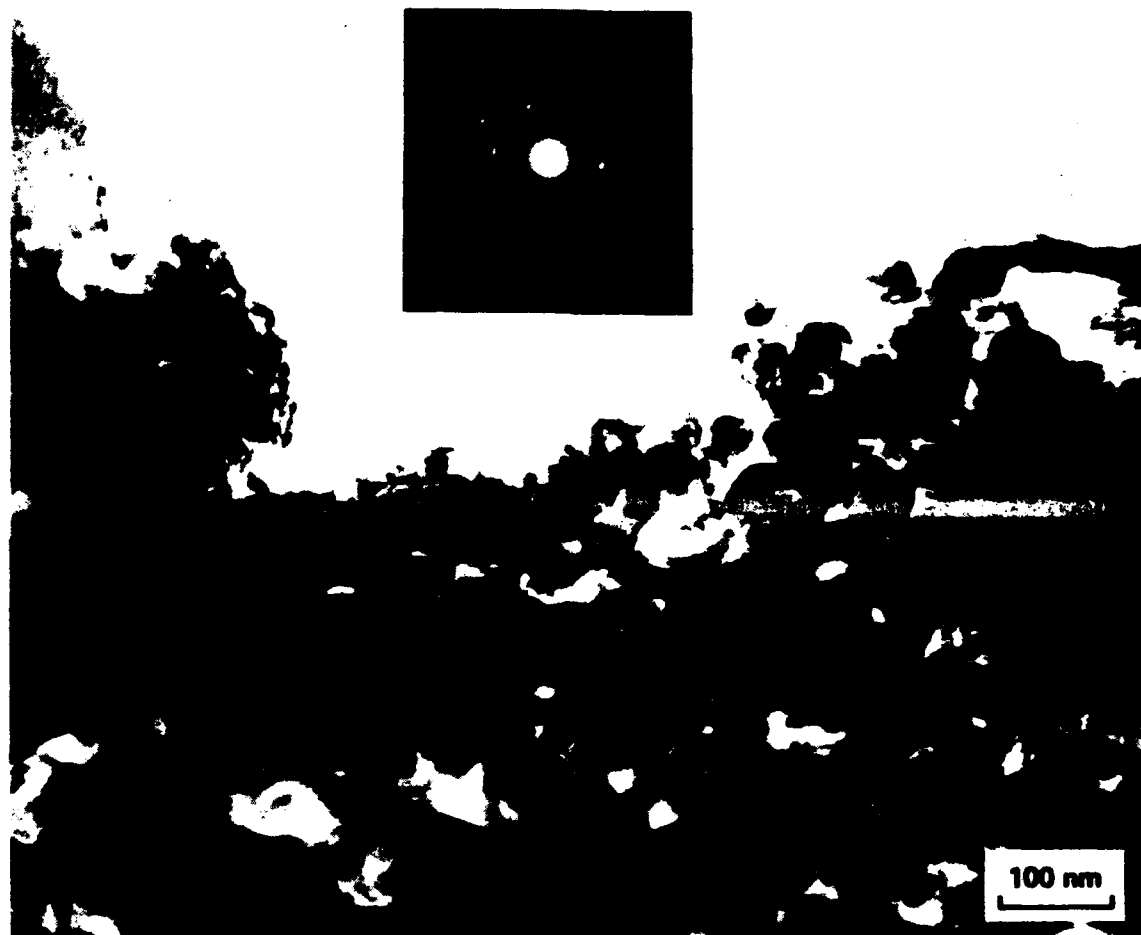
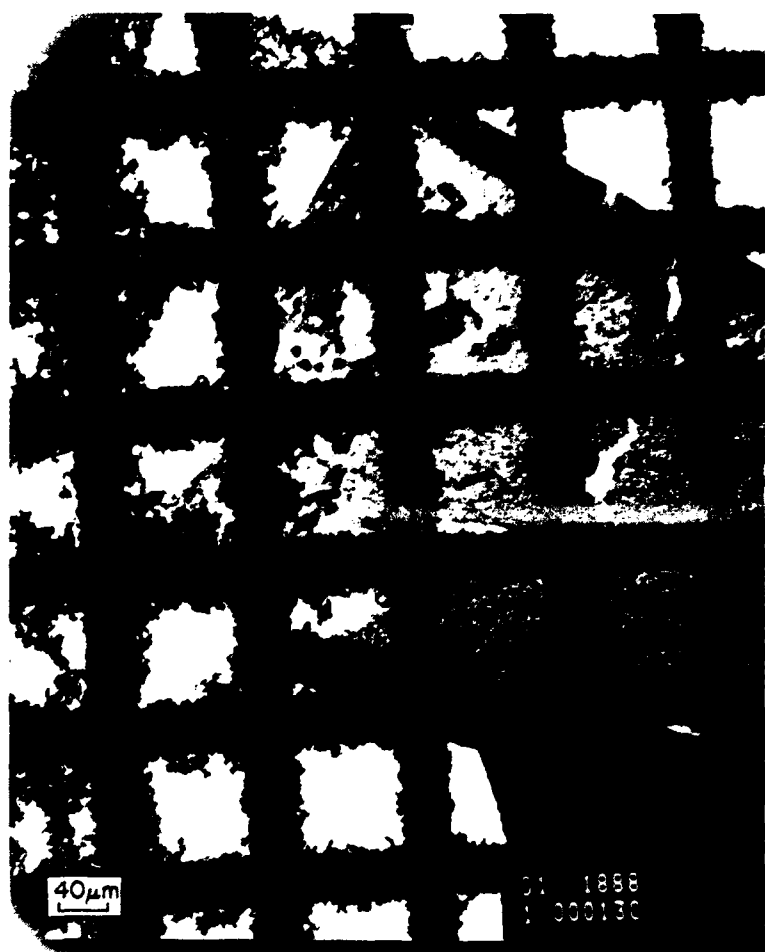


Fig. 44 Magnified view of a poly-3-methylthiophene triflate grown from 0.1M  $\text{CF}_3\text{SO}_3\text{H}$  in acetonitrile.

SC40386



**Fig. 45** TEM photograph of poly-3-methylthiophene perfluorooctylsulfonate deposited from propylene carbonate.

SC35577

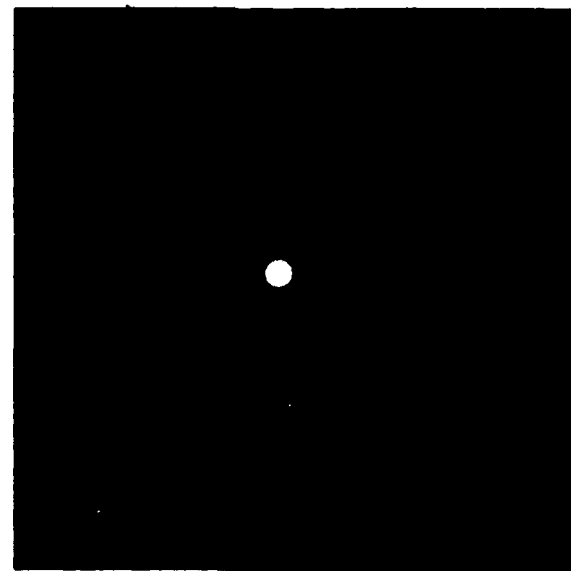
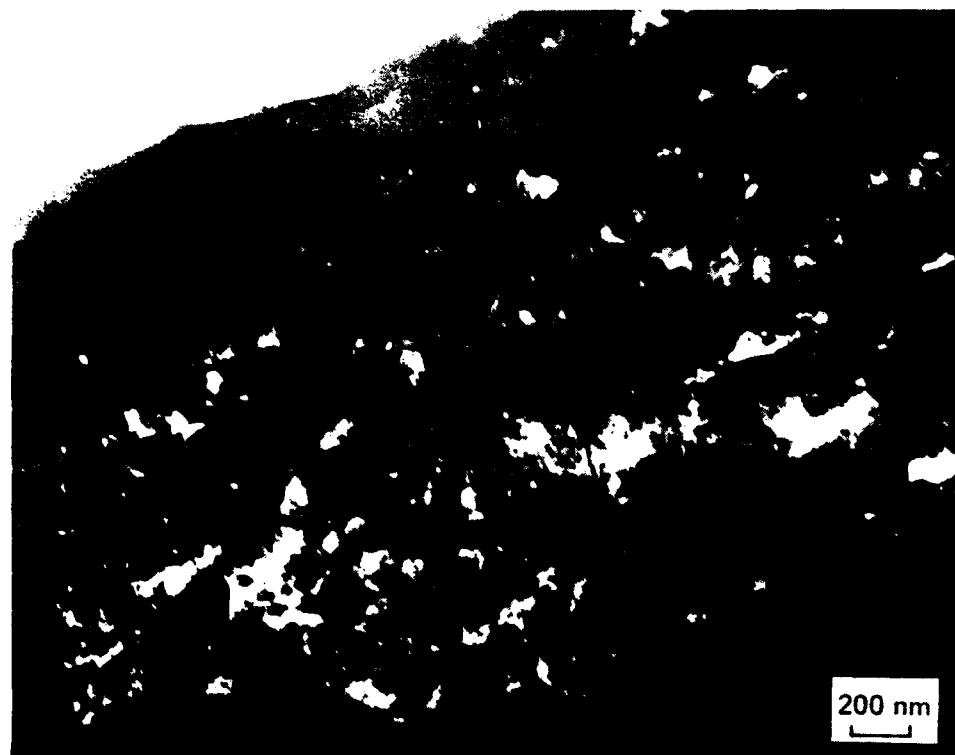


Fig. 46 Magnified view of poly-3-methylthiophene hexafluorophosphate grown from propylene carbonate.

## 4.0 REFERENCES

1. See papers appearing in "Handbook of Conducting Polymers," Vols. 1 and 2. Ed. Terje Skotheim, Marcel Dekker, Inc. (1986).
2. J. Chien, "Polyacetylene Chemistry, Physics and Materials Science," Academic Press (1984).
3. W. Wernet, G. Monkenbusch, G. Wegner, Macromol. Chem. Rapid Comm., 5, 157 (1984).
4. G.R. Mitchell, Polymer Communications, 27 346 (1986).
5. V. Schomaker, L. Pauling, J. Amer. Chem. Soc., 61, 1769 (1939).
6. R.H. Baughman, S.L. Hsu, G.P. Pez, A.J. Signorelli, J. Chem. Phys., 68, 5405 (1978).
7. H. Yashima, M. Kobayashi, K.B. Lee, D. Chung, A.J. Heeger, F. Wudl, J. Electrochem. Soc., 134, 46 (1987).
8. B.D. Cullity, "Elements of X-Ray Crystallography," Addison-Wesley Co. (1978).
9. J.A. Walker, L.F. Warren, E.F. Witucki, Patent Pending.
10. G. Tourillon, F. Garnier, J. Electroanal. Chem., 135, 173 (1982).
11. M.A. Sato, S. Tanaka, K. Kaerimama, Synth. Met., 14, 279 (1986).
12. F. Garnier, G. Tourillon, J.Y. Barraud, H. Dexpert, J. Mater. Sci., 20, 2687 (1985).

DISTRIBUTION LIST (contd.)

Report No. NADC-87092-60

	<i>No. of Copies</i>
Naval Air Systems Command .....	5
Washington, DC 20361	
Attn: Code AIR-5304C	
AIR-931A	
Office of Naval Research.....	1
800 N. Quincy St.	
Arlington, VA 22217	
Attn: Dr. Ken Wynne (Code 1113)	
Office of Naval Research, Boston .....	1
495 Summer Street	
Boston, MA 02210	

## DISTRIBUTION LIST (contd.)

Report No. NADC-87092-60

	No. of Copies
United Aircraft Corp.....	1
United Aircraft Research Labs. E. Hartford, CT 06108	
Army Materials Technology Lab .....	3
Polymers & Chemistry Div. Watertown, MA 02172	
Attn: G.L. Hagnauer R.E. Sacher C.R. Desper	
Hercules, Inc.....	2
Magna, UT 84044	
Attn: R.E. Hoffman	
University of MA .....	1
Amherst, MA 01003	
Attn: Prof. J.C.W. Chien	
Northrop Corporation .....	1
3901 W. Broadway	
Hawthorne, CA 90250	
Attn: R.L. Jones, Dept. 3870-62	
Defense Technical Information Center.....	12
Cameron Station, Bldg. 5	
Alexandria, VA 22314	
Commander.....	1
Naval Weapons Center	
China Lake, CA 92555	
Celanese Research Company .....	2
26 Main St.	
Chatham, NJ	
Attn: Dr. Paul McManon Mr. Jim Lewis	
Vought Corporation .....	1
P.O. Box 5907	
Dallas, TX 75222	
Attn: R. Knight	
NASA Headquarters .....	1
Code RV-2 (Mr. N. Mayer)	
800 Independence Ave., S.W.	
Washington, DC 20546	
Boeing Aerospace Co.....	1
P.O. Box 3999	
Seattle, WA 98124	
Attn: D. Flaherty	

## DISTRIBUTION LIST (contd.)

Report No. NADC-87092-60

	No. of Copies
Illinois Institute of Technology .....	1
Research Institute	
10 West 35th Street	
Chicago, IL 60616	
Attn: Dr. K. Hofer	
Acurex .....	1
Aerospace Systems Division	
485 Clyde Ave.	
Mountain View, CA 94042	
Attn: R.M. Washburn	
Grumman Aerospace Corp. ....	3
Bethpage, NY 11714	
Attn: J. Mahon	
L Provaromo	
Dr. R. Silberstein	
McDonnell-Douglas Corp. ....	1
P.O. Box 516	
St. Louis, MO 63166	
Attn: C. Vaccaro	
General Electric Company .....	1
Valley Forge Center	
Philadelphia, PA 19101	
Lockheed California Co. ....	1
Box 551	
Burbank, CA 91520	
Attn: Dr. R. Boschan	
General Dynamics .....	1
Convair Aerospace Division	
P.O. Box 748	
Fort Worth, TX 76101	
General Dynamics .....	1
Convair Division	
P.O. Box 1128	
San Diego, CA 92138	
Attn: P. Hertzberg	
Rockwell International Science Center .....	3
P.O. Box 1085	
Thousand Oaks, CA 91360	
Attn: P. Newman	
L Warren	
J. Walker	
NASA .....	2
Langley Research Center	
Hampton, VA 23685	
Attn: B. Stein, A. St. Clair	

DISTRIBUTION LIST

Report No. NADC-87092-60

	<i>No. of Copies</i>
B.F. Goodrich Aerospace and Defense Products .....	1
500 South Main Street	
Akron, OH 44318	
Plastics Technical Evaluation Center .....	1
ARRADCOM	
Bldg. 351-N	
Dover, NJ 07801	
Attn: A.M. Anzalone	
Massachusetts Institute of Technology .....	3
Cambridge, MA	
Attn: D. Roylance	
G. Wnek	
M. Rubner	
Rockwell International Corp.....	1
201 N. Douglas St.	
P.O. Box 92098	
Los Angeles, CA 90009	
Attn: A. Musicman	
Dept. of Mats. Sci.....	2
Pennsylvania State Univ.	
University Park, PA 16802	
Attn: Prof. B. Gordon	
Prof. J. Runt	
Dept. of Chemistry .....	1
Northwestern Univ.	
Evanston, IL 60201	
Attn: Prof. T. Marks	
NAVAIRDEVcen.....	38
Code 8131 (library) 3	
Code 6063 (Dr. L Buckley) 35	
Naval Research Laboratory.....	3
Codes 6306, 6120, 6604	
Washington, DC 20350	
Naval Surface Weapons Center .....	1
Code 234	
White Oak, Silver Spring, MD 20910	
Air Force Materials Laboratory .....	5
Wright-Patterson Air Force Base	
Dayton, OH 45433	
Attn: Codes LC (1)	
LN (1)	
LTF (1)	
LAE (1)	
MBC (1)	

END

DATE

FILMED

3 - 88

DTIC